Journal of Geodynamics 91 (2015) 51–64

Contents lists available at ScienceDirect

Journal of Geodynamics

journal homepage: http://www.elsevier.com/locate/jog

Production of mildly alkaline basalts at complex ocean ridge settings: Perspectives from basalts emitted during the 2010 eruption at the Eyjafjallajökull volcano, Iceland

Marco Viccaro[a,*], Eugenio Nicotra[a,b], Salvatore Urso[a]

[a] Università di Catania, Dipartimento di Scienze Biologiche Geologiche e Ambientali – Sezione di Scienze della Terra, Corso Italia 57, I-95129 Catania, Italy
[b] Università della Calabria, Dipartimento di Biologia Ecologia e Scienze della Terra, Via P. Bucci 15/B, I-87036 Arcavacata di Rende (CS), Italy

ARTICLE INFO

Article history:
Received 19 December 2014
Received in revised form 28 July 2015
Accepted 25 August 2015

Keywords:
Mid-ocean ridge basalt
Mantle plume
Mantle metasomatism
Metasomatic fluids
Recycling
Altered oceanic crust

ABSTRACT

The early phase of the 2010 eruption at the Eyjafjallajökull volcano (Iceland) produced poorly evolved mildly alkaline basalts that have a signature more enriched with respect to the typically depleted basalts emitted at ocean ridges. The whole rock geochemistry of these basaltic magmas offers a great opportunity to investigate the mantle source characteristics and reasons leading to this enriched fingerprint in proximity of the ocean ridge system. Some basaltic products of Katla volcano, ~25 km east of Eyjafjallajökull, have been chosen from the literature, as they display a similar mildly alkaline signature and can be therefore useful to explore the same target. Major and trace element variations of the whole rock suggest a very limited evolutionary degree for the 2010 Eyjafjallajökull products and the selected Katla magmas, highlighting the minor role played by differentiation processes such as fractional crystallization. Nevertheless, effects of the limited fractionation have been erased through re-equilibration of the major and trace element abundances at primary conditions. Concentrations of Th after re-equilibration have been assumed as indexes of the partial melting degree, given the high incompatibility of the element, and enrichment ratios calculated for each trace element. Especially for LILE (Rb, Ba, K, Sr), the pattern of resulting enrichment ratios well matches that obtained from fractional melting of peridotite bearing hydrous phases (amphibole/phlogopite). This put forward the idea that magmas have been generated through partial melting of enriched mantle domains where hydrous minerals have been stabilized as a consequence of metasomatic processes. Refertilization of the mantle has been attributed to intrusion of hydrous silicate melts and fractional crystallization of hydrous cumulates. These refertilizing melts, inherited from an ancient subducted oceanic crust, intruded into a depleted oceanic lithosphere that remained stored for a long time (hundreds of Ma or Ga) before being re-entrained in partial melting. This means that magmas could have acquired their main geochemical differences in response of the variable depletion/enrichment degree of the heterogeneous mantle portion tapped at rather shallow depth (≤100 km). Our finding is another tessera in the open debate on the plume-related vs. non plume-related origin of Icelandic magmatism.

1. Introduction

Typical magma compositions at mid-ocean ridges are chiefly confined within the field of tholeiitic basalts (N-MORBs), which are characterized by substantial depletion of LREE, LILE, HFSE, $^{87}Sr/^{86}Sr$ and $^{206}Pb/^{204}Pb$ but are enriched in $^{143}Nd/^{144}Nd$ and $^{176}Hf/^{177}Hf$ with respect to the Bulk Earth (e.g., Salters, 1996; Salters and Stracke, 2004; Stracke et al., 2005; Salters et al., 2011; Mallick et al., 2014 and references therein). Some exceptions occur at global scale, where compositions of emitted magmas display unexpected enriched signatures (E-MORBs) perhaps due to complications of the classic divergent geodynamic setting (e.g., Donnelly et al., 2004; Hemond et al., 2006). Some examples of such kind are represented by sectors of the Mid-Atlantic Ridge next to Iceland, Ascension and the triple junction of Azores, zones of the ridge separating the Cocos and Nazca plates next to Galapagos Islands or the Macquarie Ridge that marks the Australian-Pacific plate boundary south of New

* Corresponding author at: Università di Catania, Dipartimento di Scienze Biologiche, Geologiche e Ambientali – Sezione di Scienze della Terra, Volcanology Research Group, Corso Italia 57, I-95129 Catania, Italy.
E-mail address: m.viccaro@unict.it (M. Viccaro).
URL: http://www.volcanology-unict.it/ (M. Viccaro).

http://dx.doi.org/10.1016/j.jog.2015.08.004
0264-3707/

Zealand (e.g., Niu et al., 1996; Kamenetsky et al., 2000; Debaille et al., 2006; Hoernle et al., 2011; Koorneef et al., 2012).

Iceland, in particular, is the largest emerged portion above sea level of the mid Atlantic ridge system (Fig. 1a), a feature attributed by several authors to the superimposition of a hotspot that makes available considerable volumes of magma (e.g., Schilling, 1973a, 1973b, 1986; Sun et al., 1975). The Iceland Hotspot is supposed to be the surface expression of a mantle plume, whose roots could be placed at depth of about 400 km or more (Wolfe et al., 1997; Allen et al., 2002). Complexity of the Iceland geodynamic setting is confirmed by the signature of the erupted products, which display either depleted (tholeiites) or enriched (transitional to alkali basalts) signatures (see the next section for further details; e.g., Schilling, 1973a, 1973b; Sun et al., 1975; Hemond et al., 1993; Fitton et al., 1997; Gee et al., 1998; Chauvel and Hémond, 2000; Eiler et al., 2000; Skovgaard et al., 2001; Breddam, 2002; Thirlwall et al., 2004, 2006; Foulger et al., 2005; Kokfelt et al., 2006). Various models of mixing between plume-related and upper asthenospheric-related melts have been proposed by several authors to explain these characteristics (e.g., Schilling, 1973a, 1973b; Sun et al., 1975; Chauvel and Hémond, 2000; Thirlwall et al., 2004, 2006; Kokfelt et al., 2006). All these models provide evidence of marked source heterogeneity beneath Iceland, with variably depleted/enriched components tapped by mantle domains undergoing partial melting. An alternative model excludes, however, the presence of the mantle plume beneath Iceland and considers, on the basis of seismic tomography, that upwelling and thermal anomalies are limited to the upper mantle (Foulger and Anderson, 2005; Foulger et al., 2005). This model explains the great rates of magma production as due to consistent refertilization induced by recycled oceanic crust, probably associated with the Caledonian collision at 420–410 Ma and subduction of oceanic crust (closure of the Iapetus Ocean).

Iceland is therefore a unique site at global scale that offers the opportunity of investigating chemical processes at complex geodynamic settings, where mantle-derived melts bring to the surface characteristics not typical of the mid-ocean ridge system. Given their primitive character and the rather enriched signature (Sigmarsson et al., 2010; Borisova et al., 2012; Moune et al., 2012), the mildly alkaline basalts erupted during the early phase of the 2010 eruption at the Eyjafjallajökull volcano are exceptional candidates to explore this target. Elaborations presented in this work, chiefly on the basis of trace element geochemistry, improve our comprehension of the characteristics of magma production zones and offer new elements to discern the plume vs. non-plume debate for the petrogenesis of Icelandic magmas.

2. Synthesis of the geochemical features of Icelandic magmas

Comprehension of the petrological and geochemical characteristics of Icelandic magmas has been the target of several studies since about one century (e.g., Peacock, 1925, 1926). Although located in correspondence of a divergent plate boundary, magmas erupted by Icelandic volcanoes differ markedly from the typical normal mid-ocean ridge basalts (N-MORB) emitted in other sectors of the ridge and particularly in the northern sector of the mid Atlantic ridge. Two main suites of erupted products can be found in Iceland, which inherit from the mantle characteristics of depletion (tholeiites) or of various degrees of enrichment (transitional to alkali basalts).

The geochemical features of the depleted volcanic rocks of Iceland are distinct from the N-MORB, particularly in their positive Sr, Ba and Eu anomalies relative to primitive mantle (Hemond et al., 1993). On the whole, depletion is evident for most of the incompatible elements such as Rb, Th, U and K or in the lower Zr/Y for any fixed Nb/Y value (e.g., Fitton et al., 1997; Chauvel and Hémond, 2000; Kokfelt et al., 2006). Depleted lavas have low La/Sm, La/Yb, Ce/Pb but high Sm/Nd and Sr/Nd, with unradiogenic Pb ($^{206}Pb/^{204}Pb \leq 18.0$) and Sr ($^{87}Sr/^{86}Sr \leq 0.70305$) and radiogenic Nd ($^{143}Nd/^{144}Nd \geq 0.51310$) (e.g., Fitton et al., 1997; Chauvel and Hémond, 2000; Thirlwall et al., 2004; Kokfelt et al., 2006 and references therein). Anomalies of these depleted products have been interpreted as follows: (a) efficient mantle melting in the plagioclase facies (Gurenko and Chaussidon, 1995); (b) recycling in the mantle plume of oceanic gabbros (Chauvel and Hémond, 2000; Skovgaard et al., 2001; Breddam, 2002) or of the more depleted parts of a basaltic oceanic crust (Thirlwall et al., 2004); (c) contamination of primary magmas in the lower crust (Hemond et al., 1993); (d) mixing of North Atlantic upper mantle with shallow and enriched sub-continental lithosphere (Hanan and Schilling, 1997). As an alternative to the "classic" mantle plume model, Foulger et al. (2005) justify the major-trace element geochemistry and the isotope compositions of the depleted volcanic rocks as due to fractional re-melting of abyssal gabbros included in a subducted slab of oceanic crust of Caledonian age (420–410 Ma), which is now stored in the upper mantle beneath Iceland.

The enriched volcanic rocks exhibit, relative to primitive mantle, positive anomalies for Ba, Nb, Ta, LREE and negative anomalies for K and HFSE such as U, Th, Pb (Kokfelt et al., 2006 and references therein). Enriched lavas have high La/Sm, Ce/Pb, low Sm/Nd and Sr/Nd ratios; Sr and Pb in these products are radiogenic ($^{87}Sr/^{86}Sr \geq 0.70330$ and $^{206}Pb/^{204}Pb \geq 19.3$), whereas Nd is unradiogenic ($^{143}Nd/^{144}Nd \leq 0.51280$) (e.g., Fitton et al., 1997; Chauvel and Hémond, 2000; Thirlwall et al., 2004; Kokfelt et al., 2006 and references therein). The trace element and isotopic signature of these enriched products has been attributed to hypotheses contemplating contamination of the ascending magmas by hydrothermally altered Icelandic crust (Gee et al., 1998; Eiler et al., 2000) or recycling of a hydrothermally altered basaltic oceanic crust (Chauvel and Hémond, 2000; Skovgaard et al., 2001; Breddam, 2002; Thirlwall et al., 2004; Kokfelt et al., 2006). In particular, the hypotheses of recycling differ mainly in the age of the crust. Chauvel and Hémond (2000) and Skovgaard et al. (2001) argued, respectively, that the oceanic crust was recycled at ~2.7 or 3 Ga. Thirlwall et al. (2004) and Kokfelt et al. (2006) set more recent time constraints, chiefly on the basis of lead isotope systematics, at ~400 Ma (Paleozoic) and 1.5 Ga, respectively. The alternative hypothesis of Foulger et al. (2005) makes possible the presence of more alkaline products assuming that an enriched component is present in the crustal section recycled following the Caledonian subduction, and that is now stored in the mantle as enriched mid-ocean ridge basalts (E-MORB), alkali olivine basalts and related differentiates.

There is large consensus on the fact that the marked compositional variability, rather scattered on the whole island, reflects mantle domains beneath Iceland undergoing partial melting that are heterogeneous at variable scales and that magmas can be produced through sampling of depleted and enriched portions of the mantle even at the scale of a few kilometers.

3. Brief geological background of Eyjafjallajökull volcano

Eyjafjallajökull volcano arises up to 1666 m in the southwestern termination of the East Volcanic Zone (EVZ), which at present represents one of the most volcanically active regions of Iceland (Fig. 1a). EVZ is a propagating SW-NE trending rift located outside the main zone of spreading (axial rift). This area includes 30 volcanic systems that, on the whole, account for ~79% of the total volume of erupted magmas in Iceland during historical time (i.e., the last 11 centuries). However, most of the magma output is accommodated

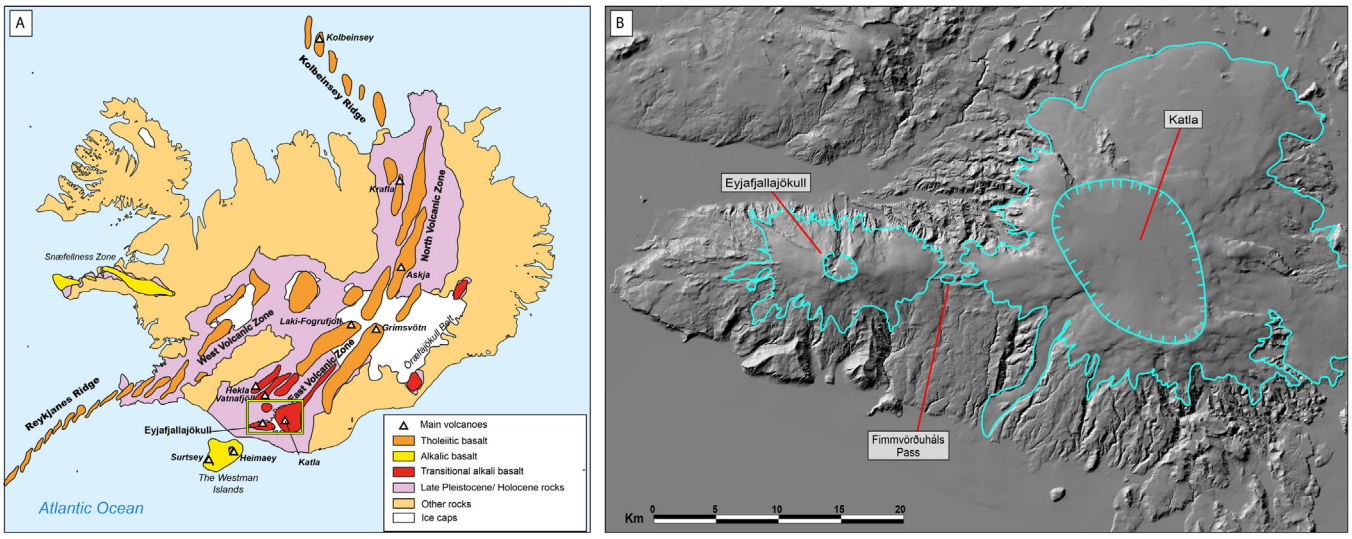

Fig. 1. (a) Sketch map of Iceland with the main suites of volcanic products emitted in the active divergent tectonics; (b) Digital Elevation Model of the Eyjafjallajökull and Katla volcanoes (source www.lmi.is/en/okeypis-kort/).

only by the four most active systems of Katla, Grimsvötn, Hekla and Bardarbunga-Veidivötn (Fig. 1a; Thordarson and Larsen, 2007). EVZ is dominated by emission of tholeiitic magmas in the northeastern segment, whereas mildly alkaline magmas characterize the southwestern segment, which is currently propagating southwesterly (Thordarson and Larsen, 2007 and references therein).

Eyjafjallajökull has been constructed through sub-glacial eruptions and its edifice is completely covered by an ice cap (Fig. 1b). It displays an irregular shape with gentle sloping flanks and a summit region characterized by a ~4-km-wide caldera opened to the north (Fig. 1b). The historical activity of Eyjafjallajökull has been characterized by long-lasting periods of quiescence, commonly broken off by initial hydromagmatic explosions evolving to eruptive episodes with Strombolian to sub-Plinian styles. The historical record includes: a radial fissure eruption dated ~920 AD, small-volume summit eruptions in 1612 AD and 1821–1823 AD, identified through chrono-stratigraphic studies and analysis of historic chronicles (Thordarson and Larsen, 2007; Dugmore et al., 2013 and references therein), and the most recent episode of 2010 AD. Extensive intrusions at 4.5 and 6.5 km of depth, whose estimated volumes are 10–17 $\times$ 10^6 m^3 and 21–31 $\times$ 10^6 m^3 respectively, occurred beneath the Eyjafjallajökull volcano in 1994 and 1999, as revealed by InSAR observations, GPS geodetic measurements, and optical tilt leveling (Pedersen and Sigmundsson, 2004, 2006; Sturkell et al., 2003; Sigmundsson et al., 2010).

All the historic eruptions of Eyjafjallajökull were more or less contemporaneous with eruptions or evidence of magma movements [i.e., glacier floods and several small earthquakes] at the nearby Katla volcano ~25 km to east (Fig. 1b; Thordarson and Larsen, 2007), probably indicating interaction of stress fields. This trend was confirmed also in coincidence of the 2010 eruption at Eyjafjallajökull, as demonstrated by several seismic swarms occurred beneath Katla in the period 2011–2012. Sturkell et al. (2003) also argued that magma movements took place at shallow levels beneath Katla in 1999 at the same time of a magma intrusion beneath Eyjafjallajökull, both evidenced by GPS and seismic data. Nonetheless, unlike the Katla volcanic system, which is much more active and known for its powerful sub-glacial eruptions, Eyjafjallajökull volcano was poorly known for a long time, and its notoriety increased only after the 2010 eruption. This event was characterized by two distinct eruptive phases: (1) an effusive flank eruption at the Fimmvörðuháls Pass on the eastern flank of Eyjafjallajökull volcano (Fig. 1b) in the period March 20 to April 12, 2010, which was characterized by emission of poorly evolved mildly alkaline basalts through lava flows and minor fountaining at the active fissure; (2) an explosive summit eruption in the period April 14 to May 22, 2010, which produced benmoreitic tephra and considerable ash fall-out that had a severe impact on air-traffic in large part of Europe (e.g., Gudmundsson et al., 2010; Sigmundsson et al., 2010; Sigmarsson et al., 2011; Borisova et al., 2012; Moune et al., 2012).

4. Sampling and analytical methods

Sixteen volcanic rock samples were collected from the lava flow field of the March–April 2010 eruption at the Fimmvörðuháls Pass, on the eastern flank of the Eyjafjallajökull volcano (Fig. 1b). Thin-polished sections have been made for petrographic and in situ microanalysis of mineral phases. Microanalytical data on olivine, plagioclase, clinopyroxene and opaque oxides found in the collected samples were obtained at the Dipartimento di Scienze Biologiche, Geologiche e Ambientali of Catania (Italy) by using a Tescan Vega-LMU scanning electron microscope equipped with an EDAX Neptune XM4-60 micro-analyzer operating by energy dispersive system characterized by an ultra-thin Be window coupled with an EDAX WDS LEXS (wavelength dispersive low energy X-ray spectrometer) calibrated for light elements. Operating conditions for the analysis of major element abundances in mineral phases were set at 20 kV accelerating voltage and 0.2 nA beam current; precision of collected data is in the order of 3–5%.

Major element compositions for the whole rock were analyzed at the Dipartimento di Scienze della Terra of Cosenza (Italy) by means of a Philips PW2404 WD-XRF on powder pellets correcting the matrix effects (Table 1). Loss on ignition was determined by gravimetric methods. REE and the other trace element abundances were determined at the SGS Laboratories of Toronto (Ontario, Canada; Table 1). Powdered rock samples were fused by Na-peroxide in graphite crucibles and dissolved using dilute HNO_3. Trace element analyses were then made by means of a Perkin Elmer ELAN 6100 inductively coupled plasma mass spectrometer. Four calibration runs were performed on international certified reference materials (USGS GXR-1, GXR-2, GXR-4 and GXR-6) at the beginning and end of the analytical run; precision is better than ~7% for all trace elements.

Table 1
Major and trace element concentrations of volcanic rocks emitted during the March–April 2010 eruption at Eyjafjallajökull volcano.

Sample	Eyja1	Eyja2	Eyja3	Eyja4	Eyja5	Eyja7	Eyja8	Eyja9	Eyja10	Eyja11	Eyja12	Eyja13	Eyja14	Eyja15	Eyja16	Eyja17	KATLA1	KATLA2
SiO_2	47.6	46.8	46.6	47.0	47.0	46.9	47.0	47.1	47.7	46.8	46.7	46.7	47.2	46.7	47.0	46.9	50.0	48.8
TiO_2	3.35	3.36	3.34	3.32	3.25	3.32	3.35	3.27	3.08	3.31	3.32	3.32	3.24	3.30	3.37	3.41	1.86	2.20
Al_2O_3	14.9	14.9	14.7	14.8	14.7	14.6	14.8	14.9	15.7	15.6	15.1	15.2	14.7	15.0	14.8	14.9	15.7	14.7
FeO_{tot}	12.1	12.6	12.6	12.3	12.3	12.5	12.3	12.1	11.4	12.2	12.4	12.3	12.1	12.4	12.5	12.5	9.6	10.9
MgO	7.49	7.84	8.16	8.12	8.18	7.98	8.13	8.07	7.50	7.26	7.89	7.83	8.39	7.97	7.92	7.82	7.62	8.56
MnO	0.21	0.22	0.22	0.21	0.21	0.22	0.21	0.21	0.20	0.21	0.22	0.21	0.21	0.21	0.22	0.22	0.16	0.17
CaO	10.2	10.4	10.4	10.3	10.3	10.4	10.3	10.2	10.1	10.5	10.4	10.5	10.1	10.3	10.2	10.4	11.6	11.6
Na_2O	3.08	3.02	2.98	3.01	3.08	3.05	2.98	3.11	3.28	3.17	3.06	3.01	3.06	3.10	3.02	2.97	2.41	2.35
K_2O	0.69	0.66	0.63	0.63	0.65	0.65	0.63	0.64	0.64	0.63	0.64	0.62	0.64	0.64	0.67	0.65	0.75	0.47
P_2O_5	0.33	0.30	0.31	0.32	0.36	0.35	0.31	0.35	0.36	0.32	0.31	0.30	0.31	0.32	0.30	0.31	0.22	0.26
Ba	165	162	151	159	152	155	156	151	154	155	155	155	156	150	160	154	119	79
Ce	48.3	45.2	42.7	44.0	42.5	42.6	45.4	44.3	43.5	44.3	43.5	43.7	44.4	44.0	46.7	48.1	28.0	20.9
Co	53.4	52.1	56.4	54.3	54.6	54.9	55.3	57.4	55.4	53.0	52.8	54.4	55.4	52.8	52.2	53.4	n.a.	n.a.
Cr	310	310	320	330	340	310	330	310	320	290	310	320	330	330	320	320	n.a.	n.a.
Dy	6.12	5.98	5.43	5.86	5.29	5.42	6.03	5.84	5.54	5.75	5.70	5.74	5.75	5.43	5.79	6.10	4.21	4.48
Er	2.95	3.00	2.82	2.95	2.80	2.77	2.91	2.97	3.01	2.90	2.88	2.92	2.95	2.67	3.02	3.15	2.41	2.33
Eu	2.26	2.28	2.21	2.17	2.10	2.18	2.29	2.20	2.11	2.16	2.27	2.16	2.29	2.22	2.29	2.41	1.47	1.33
Gd	7.08	6.80	6.46	6.58	6.52	6.24	6.58	6.62	6.58	6.85	6.60	6.64	6.76	6.63	6.74	7.37	4.71	4.13
Hf	5	5	5	5	4	4	5	4	4	5	4	4	5	4	4	5	3	3
Ho	1.19	1.16	1.12	1.16	1.14	1.17	1.15	1.10	1.14	1.17	1.13	1.13	1.18	1.12	1.18	1.23	0.88	0.85
La	20.6	20.3	18.4	19.3	18.4	18.1	19.8	19.1	18.0	18.7	19.0	18.5	19.2	18.5	19.3	21.0	11.8	8.4
Lu	0.37	0.37	0.35	0.36	0.34	0.34	0.37	0.36	0.37	0.35	0.36	0.38	0.37	0.36	0.40	0.39	0.32	0.31
Nb	16.0	15.0	20.0	20.0	13.0	16.0	17.0	15.0	19.0	18.0	16.0	13.0	20.0	13.0	14.0	15.0	13.9	10.3
Nd	28.3	27.2	26.1	26.9	26.5	25.8	27.6	26.2	25.9	26.5	27.5	25.9	27.4	27.0	28.2	28.7	16.4	13.6
Ni	202	213	231	222	231	221	216	218	211	203	216	218	238	236	217	210	n.a.	n.a.
Pr	6.54	6.50	6.04	6.14	5.90	5.81	6.34	6.08	5.91	6.16	6.35	6.08	6.22	6.14	6.34	6.82	3.66	2.84
Rb	12.5	12.1	11.3	11.3	10.9	11.0	11.6	11.4	11.0	11.4	11.3	11.6	11.8	11.1	11.7	12.5	9.9	6.5
Sc	24.0	24.0	24.0	24.0	24.0	23.0	24.0	23.0	24.0	24.0	24.0	24.0	24.0	23.0	23.0	25.0	n.a.	n.a.
Sm	6.70	6.60	6.00	6.10	6.20	5.90	6.70	6.10	6.20	6.40	6.40	6.30	6.20	6.10	6.30	7.20	4.13	3.65
Sr	470	480	470	470	470	480	480	480	480	480	470	470	460	470	460	470	304	239
Ta	1.00	1.10	1.00	1.10	0.80	0.90	1.00	0.90	1.00	1.00	1.00	1.00	1.10	0.90	1.00	1.10	0.91	0.61
Tb	1.08	1.11	1.02	1.03	1.04	0.99	1.10	1.02	1.00	1.00	1.10	1.00	1.07	1.06	1.08	1.11	0.74	0.67
Th	1.90	1.80	1.70	1.70	1.60	1.60	1.80	1.60	1.60	1.70	1.70	1.70	1.70	1.60	1.70	1.90	0.95	0.68
Tm	0.42	0.40	0.38	0.38	0.41	0.39	0.40	0.37	0.36	0.39	0.41	0.40	0.42	0.39	0.41	0.40	0.35	0.34
U	0.62	0.59	0.52	0.55	0.52	0.54	0.55	0.54	0.53	0.56	0.55	0.54	0.58	0.55	0.61	0.61	0.33	0.24
V	261	270	266	268	264	266	272	265	270	272	265	269	276	268	270	281	n.a.	n.a.
Y	28.8	28.4	26.8	27.4	26.5	26.1	28.1	27.0	26.5	26.9	27.8	27.4	27.7	26.7	28.1	29.2	n.a.	n.a.
Yb	2.50	2.50	2.20	2.30	2.20	2.10	2.40	2.40	2.30	2.30	2.20	2.40	2.50	2.30	2.40	2.60	2.13	2.00
Zr	196	186	181	183	174	182	181	181	190	190	178	183	191	177	189	191	131	104
Zr/Nb	12.3	12.4	9.1	9.2	13.4	11.4	10.6	12.1	10.0	10.6	11.1	14.1	9.6	13.6	13.5	12.7	9.4	10.1
Th/La	0.09	0.09	0.09	0.09	0.09	0.09	0.09	0.08	0.09	0.09	0.09	0.09	0.09	0.09	0.09	0.09	0.08	0.08
Ba/La	8.01	7.98	8.21	8.24	8.26	8.56	7.88	7.91	8.56	8.29	8.16	8.38	8.13	8.11	8.29	7.33	10.08	9.40
Rb/Nb	0.78	0.81	0.57	0.57	0.84	0.69	0.68	0.76	0.58	0.63	0.71	0.89	0.59	0.85	0.84	0.83	0.71	0.63
Sm/Hf	1.34	1.32	1.20	1.22	1.55	1.48	1.34	1.53	1.55	1.28	1.60	1.58	1.24	1.53	1.58	1.44	1.31	1.43
Th/Hf	0.38	0.36	0.34	0.34	0.40	0.40	0.36	0.40	0.40	0.34	0.43	0.43	0.34	0.40	0.43	0.38	0.30	0.27

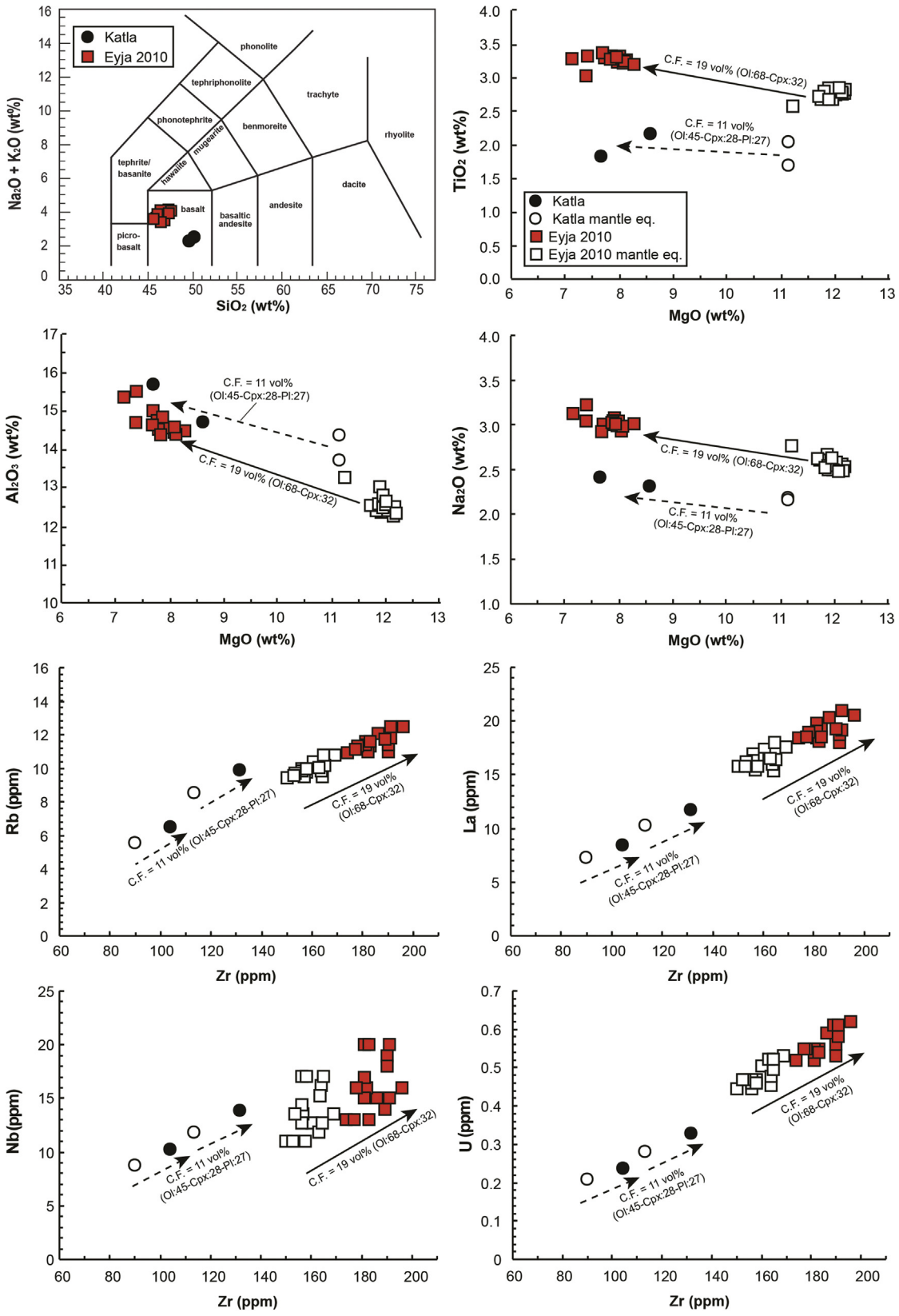

Fig. 2. Total Alkali vs. Silica (TAS; Le Maitre, 2002) diagram for the Eyjafjallajökull basalts of the 2010 eruption at the Fimmvörðuháls Pass and for two basaltic products of the Katla volcano (data from Debaille et al., 2009). Some selected major and trace elements have been plotted against MgO (wt.%) and Zr (ppm) chosen as differentiation indexes. On the same diagrams, mantle-equilibrated compositions for the same volcanic rocks have been reported (white symbols). Solid and dashed arrows indicate trends of crystal fractionation (C.F.) from mantle-equilibrated compositions for the Eyjafjallajökull and Katla products respectively (cf. also Table 2 and Table ESM1).

5. Petrography and geochemistry

Volcanic rocks erupted during the first phase of the 2010 eruption at Eyjafjallajökull volcano exhibit rather homogeneous petrographic features. Minor differences are mainly related to the groundmass texture and the relative modal abundance of mineral phases. Samples are mildly porphyritic (20–25 vol.% of phenocrysts) and highly vesiculated. Phenocrysts mostly consist of plagioclase and olivine in similar proportions, together making up 80–85 vol.% of the total phenocryst content. The mineral assemblage also includes scarce amounts of clinopyroxene (~10–15 vol.%) and opaque oxides (<5 vol.%). Plagioclase varies from medium-size crystals (up to 1.5 μm) to micro-phenocrysts (~250 μm) with composition from labradorite (An_{53}) to bytownite (An_{83}). They generally occur as euhedral crystals, tabular in shape and rather homogeneous in composition. Olivine is present as large euhedral to anhedral phenocrysts up to ~2.5 mm in size, with forsteritic contents varying at the core from Fo_{88} to Fo_{70}. Clinopyroxene mostly occurs as small euhedral phenocrysts with size ranging from 200 to 400 μm. It has been rarely found as large single crystals (up to few millimeters in size) or in aggregates with plagioclase and olivine. Compositions fall at the boundary of the augitic and pigeonitic fields on the QUAD diagram (Wo_{42-49}, En_{31-41}, Fs_{17-22}; not shown). Two types of opaque oxides have been identified with compositions either of titaniferous-magnetite or Cr-spinel. The former is from subhedral to euhedral with size up to few tens of μm, whereas the latter commonly occurs as anhedral crystals, up to 200 μm in size that are included in large olivine crystals. Glomerophyric structures involving olivine, plagioclase and clinopyroxene are also present. The groundmass has hyalopilitic to intersertal textures with plagioclase microlites predominant on other phases.

Major element compositions for bulk rock of the collected samples are reported in Table 1. In the Total Alkali–Silica diagram (TAS; Fig. 2; Le Maitre, 2002) products of the March–April 2010 eruption at Eyjafjallajökull show marked compositional homogeneity, falling in a limited area of the basaltic field and having mildly alkaline affinity. They are basaltic in composition, with SiO_2 46.6–47.7 wt.%, MgO 7.26–8.39 wt.% and limited ranges for almost all the major oxides (Table 1; Fig. 2). Only Al_2O_3 shows a more wide distribution (14.6–15.7 wt.%; Table 1; Fig. 2). Two basaltic products erupted at Katla volcano have been selected and reported in the same figure (Fig. 2; data from Debaille et al., 2009). Katla has been chosen for its proximity to Eyjafjallajökull and because erupted products display similar mildly alkaline signature. After cross-checking in the GEOROC database at the website http://georoc.mpch-mainz.gwdg.de, we have verified that only these two samples from all data available in literature for Katla display MgO contents comparable to those of our Eyjafjallajökull volcanic rocks and a complete list of rare earth and incompatible elements with good precision of the analytical data, which are therefore suitable for the petrological modeling. Although the evolutionary degree is similar, major element concentrations of the 2010 basalts erupted at Eyjafjallajökull and those of Katla differ mainly for their TiO_2, FeO and alkali contents (variations for some selected major elements are in Fig. 2; cf. Table 1). LILE and HFSE display positive correlations if Zr is taken as index of differentiation, with products of Eyjafjallajökull that have values higher than those of Katla (Fig. 2). Little variability is observed for Rb (Fig. 2), together with Ba and Sr (not shown). All the group of rare earth elements and the HFSE exhibit fairly constant concentrations at increasing Zr (e.g., La, Nb and U in Fig. 2). Rare earth and incompatible trace element abundances have been considered respectively as values normalized to the chondrite and primitive mantle compositions (Fig. 3; McDonough and Sun, 1995). The chondrite-normalized REE patterns for the Eyjafjallajökull and Katla volcanic products have similar shapes, and concentrations two order of magnitude higher than chondrite. Products of Eyjafjallajökull show higher LREE concentrations that finally result in larger HREE fractionation than Katla basalts. Concerning the incompatible trace elements, patterns of the two volcanic systems relative to the primitive mantle differ chiefly for negative anomalies of Th, U and positive anomaly of K in the products of Katla (Fig. 3; McDonough and Sun, 1995). Distribution of the normalized incompatible trace elements is rather flat with values about one order of magnitude higher than those of the primitive mantle, being intermediate between E-MORB and OIB patterns reported for comparison (Fig. 3). Compositions of other depleted (picrites and tholeiites) and enriched (alkali basalts) Icelandic products have been reported in Fig. 3 (data from Kokfelt et al., 2006). On the whole, the Eyjafjallajökull and Katla basalts considered in this paper well resemble the compositions observed for other enriched volcanic rocks erupted in Iceland that are characterized by more alkaline affinity.

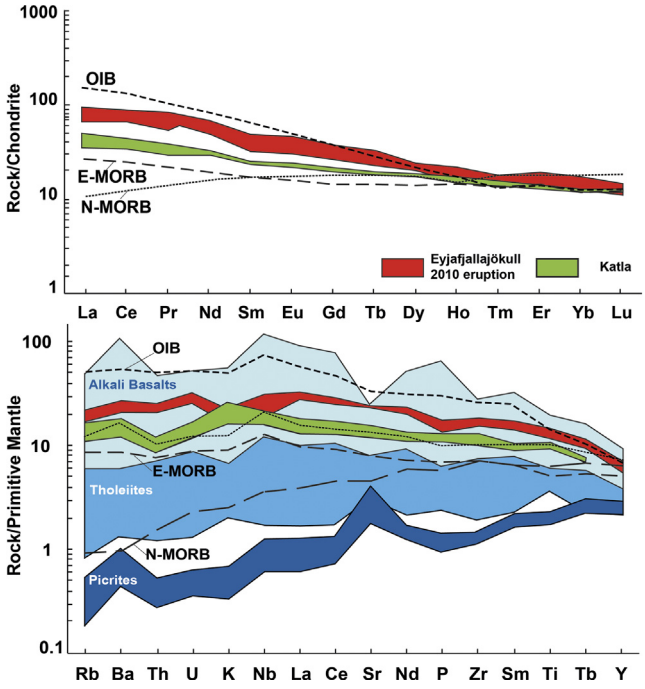

Fig. 3. REE and incompatible trace element patterns normalized respectively to the chondrite and primitive mantle compositions (McDonough and Sun, 1995) for the Eyjafjallajökull basalts of the 2010 eruption at the Fimmvörðuháls Pass and for two basaltic products of the Katla volcano (data from Debaille et al., 2009). Compositions of Icelandic picrites, tholeiites and alkali basalts have been also plotted for comparison (data from Kokfelt et al., 2006). Patterns of other suites of volcanic rocks have been reported for comparison: Normal Mid-Ocean-Ridge Basalts (N-MORB; data from Weaver, 1991), Enriched Mid-Ocean-Ridge Basalts (E-MORB; data from Donnelly et al., 2004), Ocean Island Basalts [OIB; data from Humphris and Thompson (1983), Dostal et al. (1982), Palacz and Saunders (1986), Dupuy et al. (1988), Storey et al. (1988), Weaver (1991)].

6. Discussion

6.1. Signature and evidence of modal metasomatism

The primitive basalts erupted at the Fimmvörðuháls Pass during the March–April 2010 are exceptional candidates for clarifying the mantle source characteristics of magmas emitted at the Eyjafjallajökull volcano (cf. Moune et al., 2012). Achievement of this task, through characterization of the modal mineralogy at the source of magmas, helps to explain reasons of the mildly alkaline signature and anomalous concentrations of some incompatible trace elements of these Icelandic magmas, providing new elements to evaluate the nature of the enrichment. As described above, the suite

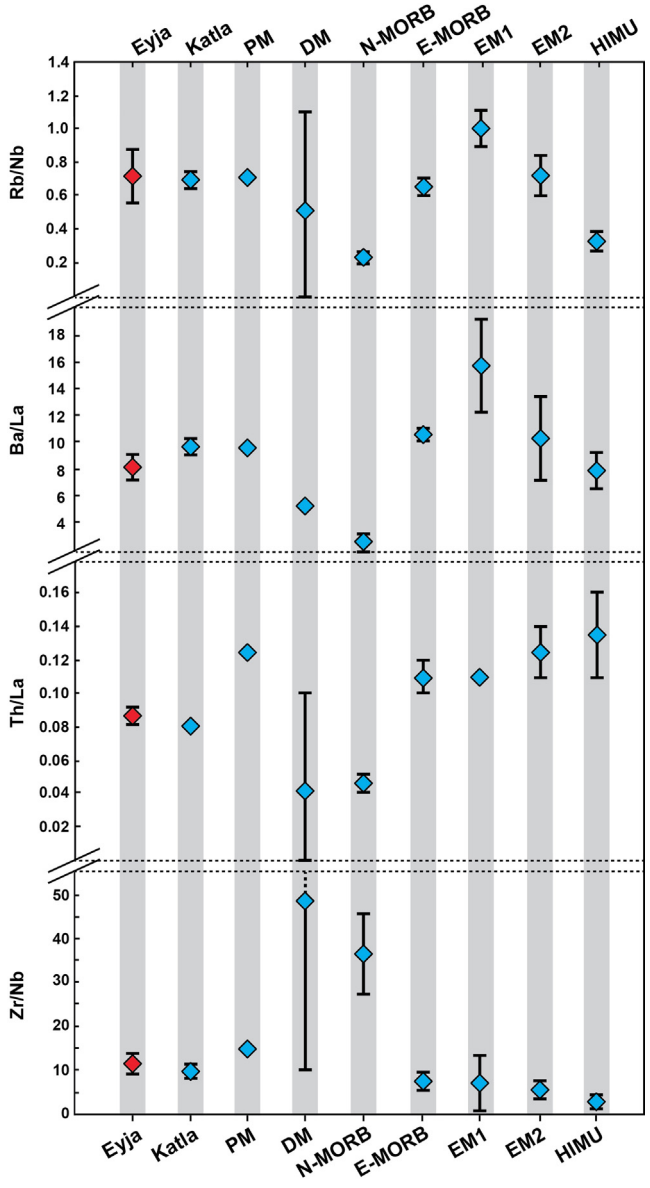

Fig. 4. Significant incompatible trace element ratios (values not normalized) for Eyjafjallajökull (red diamonds) and Katla basaltic volcanic rocks with respect to the main mantle reservoirs [Primitive Mantle (PM) from Weaver (1991); Depleted Mantle (DM) from Salters and Stracke (2004) and Willbold and Stracke (2006); Normal Mid-Ocean-Ridge Basalts (N-MORB) from Weaver (1991); Enriched Mid-Ocean-Ridge Basalts (E-MORB) from Donnelly et al. (2004); Enriched Mantle 1 (EM1) from Humphris and Thompson (1983), Storey et al. (1988), Weaver (1991); Enriched Mantle 2 (EM2) from Palacz and Saunders (1986), Dostal et al. (1982), Weaver (1991); high $^{238}U/^{204}Pb$ (HIMU) from Palacz and Saunders (1986), Dupuy et al. (1988), Weaver (1991)]. (For interpretation of the references to color in this figure legend, the reader is referred to the web version of this article.)

of basalts erupted at the Fimmvörðuháls Pass has been considered in combination with two basaltic compositions of the Katla volcanic system (from Debaille et al., 2009) in order to dispose of other compositions for the petrological elaborations. The limited variation among this suite of basalts for ratios between highly incompatible trace elements (Fig. 4) suggests that the source of magmas erupted at the Eyjafjallajökull and Katla volcanic systems, although heterogeneous, is petrologically rather similar. This feature has been extensively demonstrated also by other authors (Sigmarsson et al., 2008, 2011; Moune et al., 2012).

The rare earth and incompatible trace element patterns of the Eyjafjallajökull and Katla basalts normalized to the chondrite and primitive mantle markedly differ from the usual, depleted N-MORB fingerprint expected at ocean ridges (Fig. 3). They show together similar shapes with characteristics intermediate between those of E-MORB and OIB. The pattern of Katla basalts appears more similar to that of E-MORB, although slightly more enriched; conversely, the pattern of Eyjafjallajökull basalts resembles that of OIB, especially for its HREE fractionation (Fig. 3). Even assuming the petrological similarity of the Eyjafjallajökull and Katla sources, the distinct HREE fractionation observed in their chondrite-normalized patterns could be due to slight compositional differences in the sources and/or to limited variations of the partial melting degree. Higher degrees of enrichment and/or lower melting degrees for Eyjafjallajökull magmas could justify their higher $LREE_N/HREE_N$ ratios than those of Katla magmas. In any case, discrepancies from N-MORB of the two patterns reflect variable degrees of enrichment in the source of magmas in this region. Also ratios between incompatible trace elements show deviations from the archetypal depletion of the N-MORB magmas and more in general of the DM component, with values indicating enrichment ascribed to involvement of enriched reservoirs (Fig. 4). Processes responsible for these geochemical characteristics can be various, such as: (a) contamination by hydrothermally altered oceanic crust (Gee et al., 1998; Eiler et al., 2000); (b) deep recycling in the mantle of a hydrothermally altered basaltic oceanic crust (Chauvel and Hémond, 2000; Skovgaard et al., 2001; Breddam, 2002; Thirlwall et al., 2004; Kokfelt et al., 2006); (c) melting of an enriched oceanic crust stored in the mantle beneath Iceland (Foulger et al., 2005). Except for the first instance, dismissed however by Thirlwall et al. (2004) on the basis of Sr–Nd–Pb correlations between variably evolved volcanic rocks of Iceland, all these models imply the involvement of an altered oceanic crust (rich in fluids) in the source of the transitional/alkaline Icelandic magmas. Apart from the model favoring the influence of a mantle plume component or not for this peculiar enriched signature of the erupted magmas, we believe not reasonable that fluids remained stored in this altered oceanic crust during its subduction or else during the recycling and homogenization in the deep mantle at the scale of hundreds Ma or Ga.

We propose here that the mantle modification could be due to release of fluids from the altered oceanic crust with their intrusion in a previously depleted mantle source (MORB-like). After long storage in the mantle of this “enriched system”, magmas could have been (later) generated from domains heterogeneously refertilized as a consequence of the fluid migration. This hypothesis necessitates to the comprehensive characterization of the mantle beneath the Eyjafjallajökull and Katla volcanic systems in order to find evidence of modal metasomatism (i.e., hydrous mineral phases) and for establishing the nature of enriching fluids.

Although limited, effects due to fractional crystallization for the Eyjafjallajökull basaltic magmas were constrained by adding 19% of a mafic mineral assemblage (Table 2; Table ESM1), constituted by Fo_{88} olivine (50–68 vol.%) and clinopyroxene with Mg# 80 (32–50 vol.%), until the crystallizing olivine within the magma was equilibrated to the most forsteritic olivine found in the erupted products (Fo_{88}). This composition can be representative of equilibrium with a primary liquid generated from a mantle peridotite (Fo_{89-90}). Compositions of olivine and clinopyroxene added to the system are those observed within the basalts erupted at the Fimmvörðuháls Pass in March–April 2010, whereas trace element distribution coefficients between olivine–clinopyroxene and basaltic liquids used for calculations have been taken from the GERM database at the website http://earthref.org/KDD/ (query distribution coefficients between mineral phases and alkali basalts). The same procedure of re-equilibration at primary conditions has been done for the two basaltic products of Katla volcano. They have been equilibrated to the mantle by adding 11% of the mafic

Table 2
Compositions of the Eyjafjallajökull and Katla basaltic volcanic rocks equilibrated to mantle conditions through mass balance calculations. Mineral phase compositions and their percentages used for the mantle-equilibration have been also reported in the table.

Sample	Eyja1	Eyja2	Eyja3	Eyja4	Eyja5	Eyja7	Eyja8	Eyja9	Eyja10	Eyja11	Eyja12	Eyja13	Eyja14	Eyja15	Eyja16	Eyja17	KATLA1	KATLA2
SiO_2	46.5	45.9	45.8	46.2	46.3	46.0	46.2	46.4	46.9	45.8	45.9	45.9	46.5	45.9	46.0	45.9	49.1	48.1
TiO_2	2.80	2.80	2.78	2.77	2.70	2.76	2.79	2.72	2.57	2.77	2.76	2.76	2.69	2.75	2.81	2.84	1.70	2.05
Al_2O_3	12.6	12.5	12.4	12.5	12.4	12.3	12.5	12.6	13.3	13.1	12.7	12.8	12.4	12.7	12.4	12.5	14.4	13.7
FeO_{tot}	12.9	13.3	13.3	12.9	12.9	13.2	13.0	12.7	12.1	13.0	13.1	13.0	12.7	13.1	13.2	13.2	9.7	10.9
MnO	0.22	0.22	0.23	0.22	0.22	0.22	0.22	0.22	0.20	0.22	0.22	0.22	0.22	0.22	0.23	0.22	0.17	0.18
MgO	11.8	12.2	12.2	11.9	11.9	12.1	11.9	11.7	11.2	11.9	12.0	11.9	12.0	12.0	12.1	12.1	11.1	11.1
CaO	9.7	9.8	9.9	10.1	10.1	9.9	10.1	10.1	10.0	9.8	9.9	10.0	10.0	9.9	9.7	9.8	10.7	11.1
Na_2O	2.60	2.55	2.52	2.55	2.60	2.58	2.53	2.63	2.78	2.68	2.58	2.54	2.59	2.63	2.55	2.51	2.20	2.17
K_2O	0.58	0.56	0.53	0.53	0.55	0.55	0.53	0.54	0.54	0.53	0.54	0.52	0.54	0.54	0.57	0.55	0.68	0.43
P_2O_5	0.33	0.30	0.31	0.30	0.34	0.34	0.30	0.33	0.33	0.31	0.31	0.30	0.29	0.31	0.30	0.30	0.24	0.27
Ba	141	138	129	136	130	132	133	129	131	132	132	132	133	128	136	131	102	68
Ce	41.28	38.62	36.52	37.66	36.38	36.42	38.85	37.92	37.24	37.83	37.19	37.37	38.01	37.63	39.92	41.10	23.91	17.85
Co	77.7	77.0	79.6	73.2	73.0	78.6	75.1	76.2	73.5	80.7	75.1	77.3	73.5	73.9	75.4	78.3	n.a.	n.a.
Cr	485	481	509	537	556	489	535	509	525	442	491	506	542	527	502	498	n.a.	n.a.
Dy	5.36	5.23	4.77	5.17	4.67	4.75	5.31	5.16	4.89	5.02	5.00	5.04	5.08	4.77	5.07	5.34	3.88	3.64
Er	2.56	2.60	2.45	2.57	2.44	2.41	2.54	2.59	2.63	2.51	2.50	2.54	2.58	2.32	2.62	2.73	2.07	2.01
Eu	1.97	1.98	1.93	1.90	1.84	1.90	2.00	1.92	1.85	1.87	1.98	1.88	2.00	1.94	1.99	2.09	1.28	1.15
Gd	6.17	5.92	5.65	5.77	5.72	5.45	5.77	5.82	5.78	5.95	5.77	5.80	5.94	5.80	5.88	6.42	4.06	3.56
Hf	4.34	4.33	4.34	4.35	3.48	3.47	4.35	3.48	3.48	4.33	3.47	3.47	4.35	3.47	3.47	4.33	2.72	2.20
Ho	1.04	1.01	0.98	1.02	1.01	1.03	1.01	0.97	1.01	1.02	0.99	0.99	1.04	0.98	1.03	1.08	0.76	0.73
La	17.6	17.4	15.7	16.5	15.7	15.5	16.9	16.3	15.4	16.0	16.3	15.8	16.4	15.8	16.5	18.0	10.1	7.2
Lu	0.32	0.32	0.31	0.32	0.30	0.30	0.33	0.32	0.33	0.31	0.32	0.33	0.33	0.32	0.35	0.34	0.28	0.27
Nb	13.6	12.8	17.0	17.0	11.1	13.6	14.5	12.8	16.2	15.3	13.6	11.1	17.0	11.1	11.9	12.8	12.0	8.9
Nd	24.3	23.4	22.5	23.2	22.9	22.2	23.8	22.6	22.4	22.8	23.7	22.3	23.7	23.3	24.3	24.7	14.1	11.7
Ni	6161	7197	5741	4058	4012	6085	4156	3597	3482	8418	5650	5703	3927	5573	6288	6742	n.a.	n.a.
Pr	5.61	5.57	5.18	5.28	5.07	4.98	5.45	5.23	5.08	5.27	5.45	5.22	5.35	5.27	5.44	5.85	3.13	2.43
Rb	10.8	10.4	9.7	9.7	9.4	9.5	10.0	9.8	9.5	9.8	9.7	10.0	10.2	9.6	10.1	10.8	8.5	5.6
Sc	22.6	22.5	22.8	23.0	23.1	21.7	23.0	22.1	23.1	22.4	22.7	22.7	23.1	21.9	21.7	23.5	n.a.	n.a.
Sm	5.80	5.71	5.20	5.31	5.40	5.11	5.82	5.31	5.40	5.53	5.55	5.46	5.40	5.29	5.46	6.23	3.55	3.14
Sr	404	413	405	405	405	413	414	414	414	412	405	405	397	405	396	404	271	213
Ta	0.85	0.94	0.85	0.94	0.68	0.77	0.85	0.77	0.85	0.85	0.85	0.85	0.94	0.77	0.85	0.94	0.79	0.53
Tb	0.94	0.97	0.89	0.91	0.92	0.87	0.97	0.90	0.88	0.87	0.96	0.88	0.94	0.93	0.95	0.97	0.64	0.58
Th	1.62	1.54	1.45	1.45	1.36	1.37	1.54	1.36	1.36	1.45	1.45	1.45	1.45	1.36	1.45	1.62	0.81	0.58
Tm	0.37	0.35	0.33	0.33	0.36	0.34	0.35	0.33	0.32	0.34	0.36	0.35	0.37	0.34	0.36	0.35	0.30	0.29
U	0.53	0.50	0.44	0.47	0.44	0.46	0.47	0.46	0.45	0.48	0.47	0.46	0.50	0.47	0.52	0.52	0.28	0.21
V	269	275	279	290	287	277	293	290	295	272	277	281	302	283	279	288	n.a.	n.a.
Y	24.5	24.1	22.8	23.3	22.5	22.2	23.9	23.0	22.5	22.9	23.6	23.3	23.5	22.7	23.9	24.8	n.a.	n.a.
Yb	2.19	2.19	1.93	2.03	1.94	1.84	2.11	2.12	2.03	2.01	1.93	2.11	2.21	2.02	2.10	2.28	1.85	1.73
Zr	169	160	156	158	150	157	156	156	164	164	153	158	165	153	163	165	113	90
Total solid added (vol.%)	19	19	19	19	19	19	19	19	19	19	19	19	19	19	19	19	11	11
Ol (vol.%)	12.0	12.0	11.0	10.0	9.5	11.0	10.0	9.5	9.5	13.0	11.0	11.0	9.5	11.0	11.0	12.0	7.2	7.1
Cpx (vol.%)	7.0	7.0	8.0	9.0	9.5	8.0	9.0	9.5	9.5	6.0	8.0	8.0	9.5	8.0	8.0	7.0	2.3	2.4
Pl (vol.%)	0.0	0.0	0.0	0.0	0.0	0.0	0.0	0.0	0.0	0.0	0.0	0.0	0.0	0.0	0.0	0.0	1.0	1.2
Ti–Mt (vol.%)	0.0	0.0	0.0	0.0	0.0	0.0	0.0	0.0	0.0	0.0	0.0	0.0	0.0	0.0	0.0	0.0	0.5	0.3

Composition of added mineral phases (wt.%)

	Ol	Cpx	Ti–Mt	Pl
SiO_2	40.0	52.6	0.4	48.3
TiO_2	0.16	n.a.	18.80	n.a.
Al_2O_3	0.1	3.2	4.5	32.7
Fe_2O_3	11.52	7.38	63.18	0.73
FeO	0.2	0.3	0.6	n.a.
MgO	46.7	16.2	4.9	0.2
CaO	0.31	19.93	n.a.	15.71
Na_2O	0.31	0.38	n.a.	2.07
K_2O	0.11	n.a.	n.a.	0.21
P_2O_5	0.5	n.a.	n.a.	n.a.

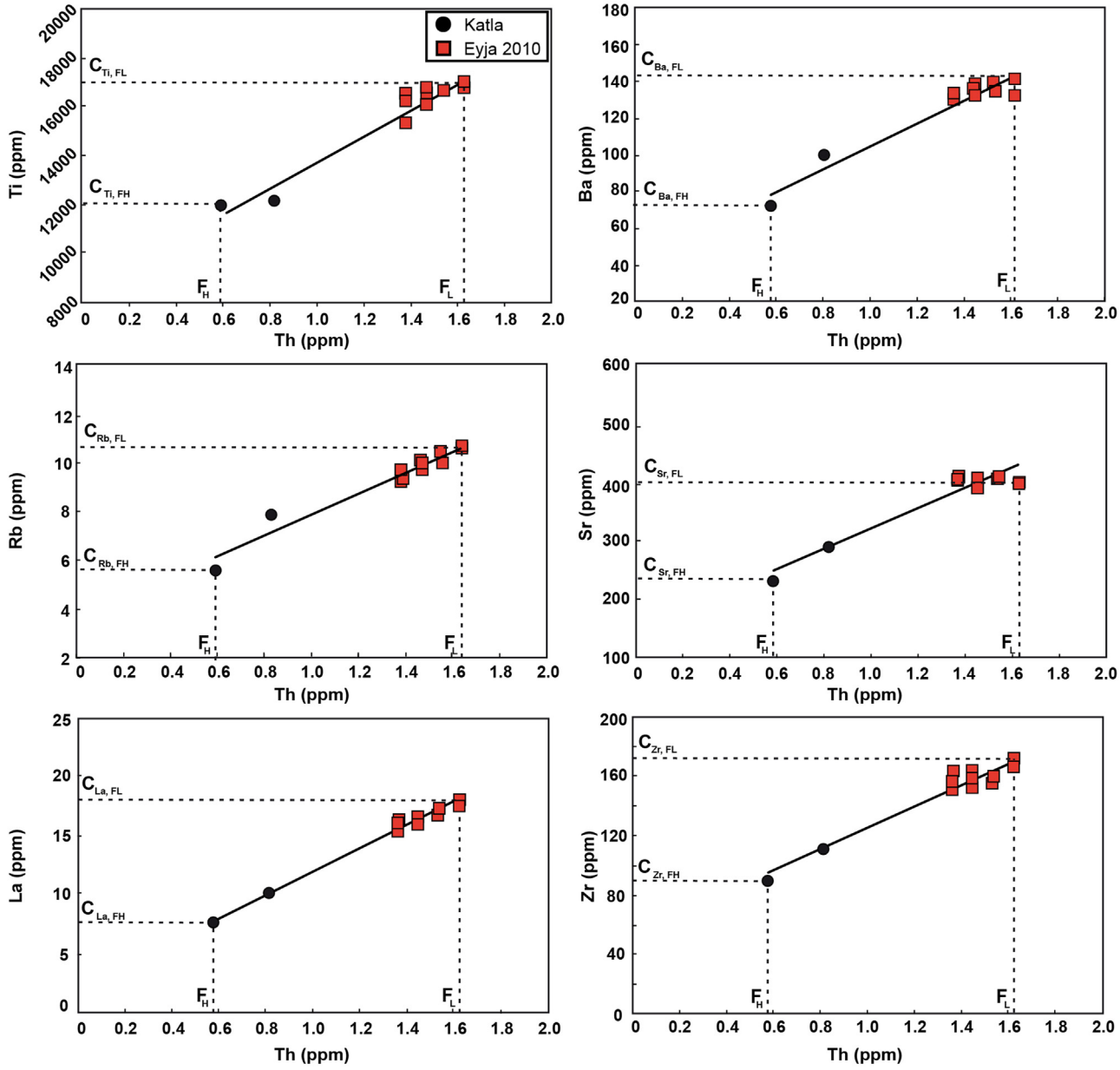

Fig. 5. Selected incompatible elements vs. Th as an index of partial melting degrees (F) for mantle-equilibrated compositions of the Eyjafjallajökull and Katla basalts. C_{FL} and C_{FH} for the other trace elements have been respectively estimated for low and high degrees of melting through simple bivariate linear regression. See text for discussion.

assemblage, given their evolutionary degree lower than that of Eyjafjallajökull products.

Supplementary material related to this article can be found, in the online version, at http://dx.doi.org/10.1016/j.jog.2015.08.004.

After equilibration to mantle conditions, concentrations of highly incompatible elements of these theoretic liquids can be assumed as indexes of the partial melting degree (F). Specifically, high and low concentrations of elements characterized by $D < 0.001$ reflect, respectively, low (F_L) and high (F_H) degrees of melting. Based on this, an enrichment ratio (E_i) for each incompatible element i can be calculated; E_i depends on the distribution coefficient (D) of the element i and for highly incompatible elements approximates the value given by F_H/F_L (cf. Class and Goldstein, 1997). The original method was applied by these authors to a co-genetic suite of magmas (i.e., derived from a single source), where equilibrated incompatible trace elements show linear trends on element-element plots. The Eyjafjallajökull and Katla magmas are not co-genetic, however they present geochemical similarities that suggest their derivation from a common event of enrichment occurred in the mantle source. Differences observed for the Eyjafjallajökull and Katla magmas in the incompatible trace element ratios or the normalized trace element patterns to the primitive mantle should be therefore ascribed to heterogeneity related to the enriching episode or to slight differences in the degree of partial melting. In this regard, many authors discussed how heterogeneity in the upper mantle can affect the degree of partial melting and the composition of primary magmas (e.g., Albarede, 1992; Niu et al., 2001, and references therein). Indeed, the partial melting degree (F) can be assumed as a function of three main parameters: (1) the mantle source composition (X); (2) the thermal regime (T); (3) the pressure at which partial melting occurs (P). Looking at a regional scale, T and P for the production of Eyjafjallajökull and Katla magmas could be reasonably assumed similar, i.e., the thermal anomaly and the depth at which mantle starts to melt can be assumed

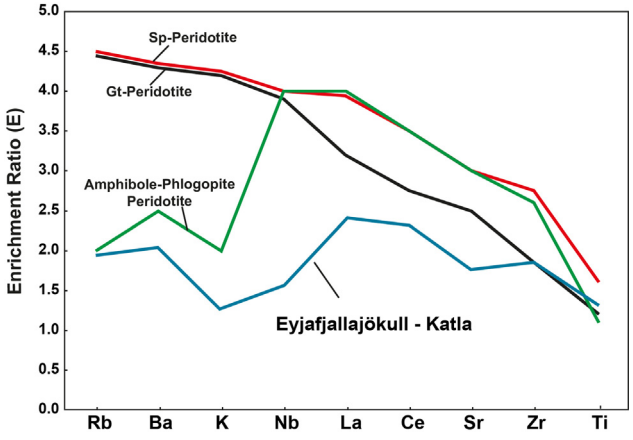

Fig. 6. Enrichment ratio (E_i) patterns for spinel (sp), garnet (grt) and hydrous-phase bearing peridotites (amphibole and phlogopite). E_i for each trace element has been obtained considering $C_{i,FL}/C_{i,FH}$, with $C_{i,FL}$ (concentration of the i element at low degree of fractional melting F_L) and $C_{i,FH}$ (concentration of the i element at high degree of fractional melting F_H) derived through simple linear regression on bivariate diagrams. The inferred mineral modal proportions of the used peridotite are the following: spinel peridotite ol:opx:cpx:sp = 58:30:10:2; garnet peridotite ol:opx:cpx:grt = 60:25:9:6; hydrous phase-bearing-peridotite ol:opx:cpx:grt:phl:amph = 73:22:3:1:1. Distribution coefficients used for fractional melting the peridotites are the following: olivine, orthopyroxene, clinopyroxene, spinel and garnet from Beattie (1993a, 1993b), Hart and Dunn (1993), Kelemen et al. (1993); amphibole and phlogopite from Adam et al. (1993), Irving and Frey (1984), LaTourrette et al. (1995). E_i pattern for the Eyjafjallajökull volcanic rocks well resembles that obtained from fractional melting of hydrous phase-bearing peridotites.

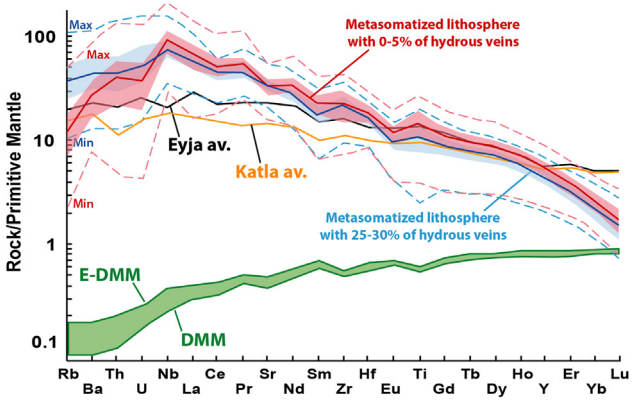

Fig. 7. Average incompatible trace element abundances of Eyjafjallajökull (black solid line) and Katla (orange solid line) basalts normalized to the primitive mantle (McDonough and Sun, 1995) plotted together with the pattern deriving from melting of a lithosphere metasomatized through the intrusion of different amounts of veins bearing cumulates of hydrous minerals (red lines = 0–5% and cyan lines = 25–30% of trapped liquid; cf. Pilet et al., 2011 for details on the starting compositions used in the modeling). The partial melting degree of the hydrous cumulate in the veins has been assumed to be 50% in both cases. The red and cyan bands indicate the corresponding $\pm 1\sigma$ variation, whereas dashed lines represent the maximum and minimum compositions calculated (cf. Pilet et al., 2011). The green band is referred to depleted MORB mantle (DMM) and slightly enriched DMM compositions (data from Workman and Hart, 2005). See text for discussion. (For interpretation of the references to color in this figure legend, the reader is referred to the web version of this article.)

comparable. Conversely, changes of mantle source composition X, which could depend on variable degrees of metasomatic enrichment, affect the degree of partial melting even at similar T and P. This means that concentrations of incompatible trace elements for equilibrated magmas produced from a heterogeneous source depend on both X and F. Viccaro and Cristofolini (2008) demonstrated that the enrichments ratio's method holds true even in the presence of a heterogeneous mantle source, assuming that the source has similar petrological characteristics before the metasomatic input and that the enriching event is the same (although with different proportions). Under these conditions, the methodological approach leads to the identification of trace elements more compatible in residual minerals in the magma source, as they are less enriched at low melting degrees. Given its marked incompatibility in basaltic systems either in the presence of fluids in the source or not, Th has been chosen as index element for the enrichment ratio calculation. On the basis of $C_{Th,FL}/C_{Th,FH}$, E_{Th} is ~2.5. Enrichment ratios for the other trace elements were estimated through simple linear regressions on Harker diagrams with C_{Th} at F_L and F_H as indexes (Fig. 5). Discrepancies for some elements from a perfect regression passing through the origin is due to the fact that element concentrations depend not only on F but also on X. The resulting pattern of enrichment ratios for some incompatible elements is shown in Fig. 6. Negative anomalies are evident for LILE (Rb, Ba, K, Sr) with respect to some HFSE and REE (Nb, Zr, La, Ce). These negative anomalies characterize elements highly incompatible for typical mantle minerals such as olivine, orthopyroxene, clinopyroxene, spinel, garnet. Indeed, the resulting pattern referred to the Eyjafjallajökull and Katla magmas are markedly different from those obtained by fractional melting of spinel- or garnet-peridotites (Fig. 6). This means that other phases retaining preferentially LILE are present in the magma source region of the Eyjafjallajökull and Katla volcanic systems. The pattern of enrichment ratios obtained for these magmas has been also compared with that calculated for fractional melting of a peridotite bearing hydrous phases such as amphibole/phlogopite (Fig. 6). The resemblances observed are indication for the occurrence of residual hydrous minerals such as amphibole and phlogopite in the magma source of Eyjafjallajökull and Katla volcanoes. This evidence might support the idea that magmas have been generated through partial melting of mantle domains where these hydrous minerals have been previously stabilized as a consequence of metasomatic enrichment.

Evidence of metasomatism in mantle peridotites generally manifests as intruded veins with glass and cumulates that are the result of fractional crystallization in the range 1.5–3 GPa of H_2O–CO_2-rich melts within the lithosphere (Morris and Pasteris, 1987; Nielson and Noller, 1987; Wilshire, 1987; Harte et al., 1993; Nielson and Wilshire, 1993; Downes, 2007). Compositions of the melts producing the metasomatic veins in the lithosphere are scarcely constrained worldwide, although they are supposed to be low-degree melts (degree of melting from 0.2 to 2 wt.%) deriving from systems where large amounts of H_2O and CO_2 are available (i.e., altered oceanic crust, enriched mantle peridotites, etc.). During the ascent and fractional crystallization, these low-degree partial melts produce a large spectrum of mineral assemblages ranging from anhydrous veins (chiefly pyroxenites with or without garnet) to hydrous veins (mostly pyroxenites with amphibole and phlogopite) enriched in highly incompatible elements (Morris and Pasteris, 1987; Nielson and Noller, 1987; Wilshire, 1987; Bodinier et al., 1990; Harte et al., 1993; Nielson and Wilshire, 1993). Liquids from partial melting at high degrees (>20%) of hydrous veins in metasomatized lithosphere have been acknowledged to be significant components in the sources of alkaline magmas emitted at oceanic and continental settings, because they have trace element concentrations largely comparable to those of several alkali basalts (e.g., Pilet et al., 2008, 2011 and references therein). In Fig. 7 trace element abundances of Eyjafjallajökull and Katla basalts normalized to the primitive mantle (McDonough and Sun, 1995) have been plotted together with the pattern deriving from melting of a metasomatized lithosphere intruded by veins bearing cumulates of hydrous minerals (cf. Pilet et al., 2011). The starting composition used in the model of Pilet et al. (2011) corresponds to a metasomatized lithosphere, whose enrichment manifests as 0–5% and 25–30% of entrapped liquid within the peridotite, simulating respectively

low and high degrees of metasomatic enrichment. In the model, the used liquid composition underwent 47–80% of fractionation (L_2 of Pilet et al., 2011), leaving glass plus a hydrous cumulate primarily constituted of amphibole, clinopyroxene, phlogopite, plagioclase and other accessory mineral phases [see Figs. 5 and 7 from Pilet et al. (2011) for further details on the starting compositions and other parameters of the modeling]. Compositions of the liquids represented in Fig. 7 have been obtained at 50% of partial melting degree of the hydrous cumulate. The average compositions of Eyjafjallajökull basalts exhibit elemental anomalies (i.e., Rb, Ba, Th, U, LREE, Zr, Hf, MREE) and slopes relative to the primitive mantle compositions that are markedly similar, except for Nb and HREE, to those of the modeled metasomatized source with 25–30% of hydrous veins. This supports the idea that an important amount of metasomatic veins bearing hydrous mineral phases (intruded in a depleted lithosphere) could be an essential component in the petrogenesis of Eyjafjallajökull magmas (Fig. 7). Differences observed for Nb and HREE, observed also in other OIB volcanics (cf. Pilet et al., 2011), could be influenced by the proportion of hydrous minerals (amphibole and phlogopite) participating to melting: with reference to basaltic liquids, amphibole has distribution coefficients >1 for MREE and HREE and slightly <1 for Nb, whereas REE in phlogopite have generally $K_D < 1$ (with HREE less incompatible) and ${}^{Phl/melt}K_{DNb} \geq 1$ (Arth, 1976; Green and Pearson, 1985). This might reflect proportions of residual phlogopite higher than amphibole in the source of magmas. The average compositions of Katla basalts show a trace element pattern normalized to the primitive mantle very similar to that of Eyjafjallajökull magmas, although at lower values for all the displayed elements (Fig. 7). With respect to the Eyjafjallajökull pattern, Th of Katla magmas exhibits a more pronounced negative anomaly, Nb with a slightly positive anomaly and La with no positive anomaly. On the whole, the pattern of Katla basalts has elemental anomalies and slopes that are more similar to those of a modeled metasomatized lithosphere with 0–5% of veins bearing hydrous mineral phases. This could mean that, although present, the metasomatic contribution to the petrogenesis of Katla magmas is lower than that of Eyjafjallajökull magmas.

6.2. Nature of enriching agents

Introduction of oceanic crust and sediments via subduction is one way to modify the chemistry of the mantle and to contribute to its chemical and isotopic heterogeneity at various timescales (e.g., Hofmann and White, 1982; Zindler and Hart, 1986; Niu and O'Hara, 2003; Tatsumi and Kogiso, 2003). The oceanic crust undergoing hydrothermal modification and weathering is altered and becomes rich in elements such as K, Rb, Cs, U and to a lesser extent Ba (e.g., Hart and Staudigel, 1982; Staudigel et al., 1995, 1996), whereas Th, Pb and greater amounts of Ba are generally provided by sedimentary components (McCulloch and Gamble, 1991). Altered oceanic crust and sediments are therefore able to carry at depth a conspicuous load of fluids and elements extraneous to the classical mantle system. The altered oceanic crust dehydrates during subduction and releases part of fluid mobile elements such as K, Ba, Rb, Cs and to a minor extent U, Sr and Pb, whereas less mobile elements such as Th, Nb, Zr, Hf, MREE and HREE are kept almost entirely into the slab (e.g., Hart and Staudigel, 1982; Staudigel et al., 1995, 1996; Becker et al., 2000). This means that not all the "crustal" elements can be introduced in the deeper parts of the mantle.

The occurrence of modal metasomatism in the source of Eyjafjallajökull and Katla magmas implies a two-stage history of the mantle before production of melts with enriched signature. A first stage of fluid release from the altered oceanic crust component should have led to refertilization and stabilization of the metasomatic mineral phases with enrichment in key elements; a second stage denotes participation of hydrous minerals to partial melting and

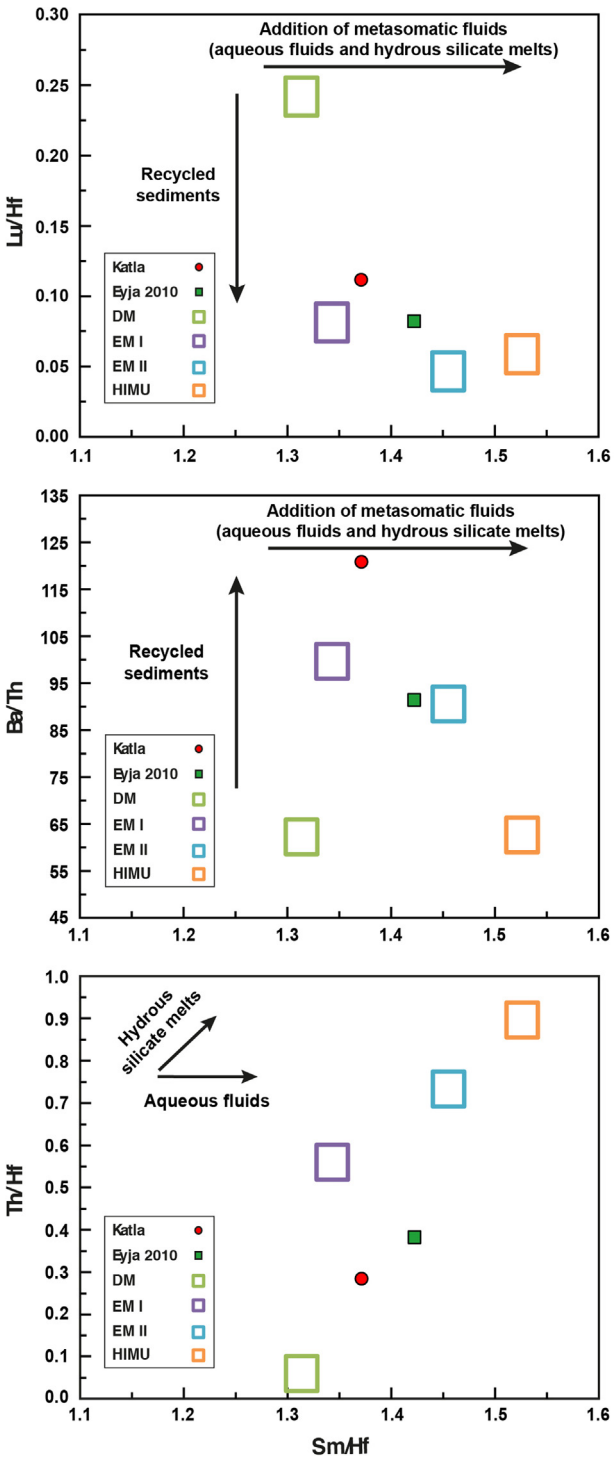

Fig. 8. Lu/Hf–Ba/Th–Th/Hf vs. Sm/Hf diagrams for average compositions emitted at Eyjafjallajökull during the early phase of the 2010 eruption and average of the chosen basaltic samples for Katla volcano (data source from Debaille et al., 2009). Data source used for the average ratios relative to the depleted and enriched mantle components reported in the diagrams are the same as in Fig. 4.

generation of enriched magmas. Understanding the nature of the earlier enriching event is therefore one of the key issues for casting light on the geodynamic significance of the enrichment itself.

A good method for interpreting the characteristics of enriching fluids is the use of ratios between elements having diverse affinity depending on the type of metasomatic fluid (i.e., hydrous silicate melts, supercritical and aqueous fluids). In this regard,

X/Hf elemental ratios are among the best indicators, where X is a trace element selected for its particular mobility or incompatibility referred to Hf. Elements such as Sm, Nd, Ba and Hf are similarly incompatible during partial melting, which means that effects of source depletion on Sm/Hf, Nd/Hf, Ba/Hf ratios are expected to be rather low. Nevertheless, Sm, Nd, Ba are generally more enriched in all the types of metasomatic fluids than Hf; therefore high X/Hf elemental ratios may be attributed to selective addition of Sm, Nd or Ba by fluids (e.g., Mysen, 1979; Spera et al., 2007; Elliott et al., 2007 and references therein). The behavior of Sm–Th–Hf in presence of low-temperature fluids (aqueous fluids) or high temperature fluids (hydrous silicate melts) is different and therefore useful to discern the fluid characteristics. Various authors demonstrated that aqueous fluids transport Sm but not Th and Hf, whereas hydrous silicate melts bring Sm and to various extents also Th, but not Hf (e.g., Mysen, 1979; McDade et al., 2003; John et al., 2004; Spera et al., 2007; Elliott et al., 2007; Viccaro et al., 2011 and references therein). This means that aqueous fluids keep the Th/Hf ratio almost constant, whereas hydrous silicate melts produce concordant increase of Sm/Hf and Th/Hf. Diagrams of Fig. 8 report compositions of the Eyjafjallajökull and Katla basalts for elements having variable affinities with hydrous silicate melts and aqueous fluids. These have been plotted within the context of depleted mantle components (DM and N-MORB) and other mantle reservoirs (EM1-EM2-HIMU) interpreted as recycling of sediments or ancient oceanic crust (e.g., Hofmann, 1997; Stracke et al., 2003, 2005). Various studies provided, however, substantiations that a large range of Sr–Nd–Pb isotopic compositions (from enriched mantles to HIMU) can be produced if metasomatized lithospheric mantle is isolated for timescales in the order of 1–2 Ga (Workman et al., 2004; Pilet et al., 2011). Specifically, Workman et al. (2004) invoked a model for the origin of the EM2 component through metasomatic enrichment of oceanic lithosphere and long-term storage (scale of Ga) in the mantle. The Sm/Hf ratio is not altered significantly through sediment recycling (EM1), whereas it increases with involvement of fluids inherited from EM2 or HIMU components (Fig. 8). Sediments contribute in the extreme depletion of Lu/Hf and enrichment of Ba/Th at rather similar Sm/Hf, whereas metasomatic fluids can variably increase either Sm/Hf or Ba/Th depending on their nature and composition (Fig. 8). In this regard, concordant variations of Sm/Hf and Th/Hf provide substantiations for the involvement of hydrous silicate melts during magma production (Fig. 8). As shown above, these hydrous silicate melts could represent the metasomatizing agent in form of hydrous veins that intruded the depleted oceanic lithosphere (Fig. 8).

7. Implications and conclusions

Our findings imply a two-stage history that led firstly to refertilization of the mantle beneath Eyjafjallajökull and Katla volcanoes and then to its partial melting and production of enriched magmas. The presence of metasomatic phases, participating to melting but left residual in the mantle, indicates that a previous event of enrichment should have occurred, because stabilization of hydrous phases and their partial melting cannot be coincident. Refertilization has been attributed to mobilization of hydrous silicate melts inherited from a subducted altered oceanic crust that modified an oceanic lithosphere with depleted signature. This refertilized system could have been then stored in the mantle at the scale of Ma/Ga in order to develop the isotopic signature in part comparable to that of enriched mantle components (cf. Chauvel and Hémond, 2000; Thirlwall et al., 2004; Foulger et al., 2005; Kokfelt et al., 2006). Support for a two-stage history of the mantle could derive from the fact that dehydration of the altered oceanic crust during subduction releases early a large load of fluid mobile elements in variable proportions (K, Ba, Rb, Cs, U, Sr and Pb), which can hardly reside in the slab for long time during and after the subduction. These fluids are therefore responsible for the stabilization of hydrous minerals within metasomatic veins intruded in a depleted mantle.

In addition to Eyjafjallajökull and Katla volcanic systems, also other parts of Iceland (i.e., the Snaefellness peninsula, the Oraefajökull belt, other sectors of the East Volcanic Zone and the Westman Islands; Fig. 1a) are characterized by emission of variably differentiated transitional to alkaline products with geochemical fingerprints that can be ascribed to derivation from enriched mantle sources. The main models proposed to explain the enrichment of Icelandic magmas invoke the presence of a mantle plume that recycles an ancient hydrothermally altered oceanic crust and interacts with the Mid Atlantic Ridge beneath Iceland (e.g., Schilling, 1973a, 1973b; Sun et al., 1975; Chauvel and Hémond, 2000; Thirlwall et al., 2004, 2006; Kokfelt et al., 2006). Alternatively, magma overproduction and emplacement could be due to events of refertilization triggered by recycling of an altered oceanic crust subducted at 420–410 Ma during the closure of the Iapetus Ocean (Foulger and Anderson, 2005; Foulger et al., 2005). Both these cases imply the presence of a chemical (but in some way also physical) anomaly in the mantle beneath Iceland, where an altered oceanic crust contributes to the enrichment. Our data support the idea that this enriching component is a metasomatized oceanic lithosphere bearing veins of hydrous silicate melts and their related cumulates. On the whole, the isotope systematics obtained on variably enriched Icelandic volcanic rocks set constraints for subduction of oceanic crust, metasomatism of the mantle and recycling processes with timescales of hundreds of Ma or Ga. Among the possible processes, our model includes: (a) dehydration and fluid release from an ancient slab; (b) refertilization of depleted mantle domains by means of fluids; (c) stabilization of metasomatic minerals precipitating from hydrous silicate melts; (d) storage for long time in the mantle in order to develop the observed isotopic evolution; (e) involvement in the partial melting of variably enriched, heterogeneous mantle domains and magma production. This means that the geochemical signature of Icelandic magmas is mostly acquired at "shallow" depth ($\leq$100 km), where the thermal regime of the ocean ridge and of a more deep-seated thermal anomaly ($\leq$400 km) are able to produce melting of scarcely homogenized mantle domains. Magmas inherit compositional differences due to the variable depletion/enrichment degree depending on the mantle portions tapped, which testify heterogeneity even at the scale of few kilometers. Our model has the advantage to include either the enriched or depleted components in the metasomatized oceanic lithosphere. Although other elements are necessary for the verification of our hypothesis, these results add useful hints of reflection to the debate of broad-interest on the plume vs. non-plume origin of Icelandic magmatism.

Acknowledgements

Field-work and part of the analytical results presented in this study have been made possible through financial support from the University of Catania (Italy) to Marco Viccaro. Giancarlo Niceforo is greatly thanked for having given kind assistance for the XRF analyses at the University of Calabria. Comments, suggestions and corrections provided by the Editor W.P. Schellart, and the reviewers S. Mallick and C. Manning helped to improve quality and clarity of this paper.

References

Adam, J., Green, D.H., Sie, S.H., 1993. Proton microprobe determined partitioning of Rb, Sr, Ba, Y, Zr, Nb and Ta between experimentally produced amphiboles and silicate melts with variable F content. Chem. Geol. 109, 29–49.

Albarede, F., 1992. How deep do common basaltic magmas form and differentiate? J. Geophys. Res. 97 (B7), 10997–11009.
Allen, R.M., Nolet, G., Morgan, W.J., Vogfjord, K., Bergsson, B.H., Erlendsson, P., Foulger, G.R., Jakobsdottir, S., Julian, B., Pritchard, M., Ragnarsson, S., Stefansson, R., 2002. Imaging the mantle beneath Iceland using integrated seismological techniques. J. Geophys. Res.: Solid Earth 107, http://dx.doi.org/10.1029/2001JB000595.
Arth, J.G., 1976. Behavior of trace elements during magmatic processes – a summary of theoretical models and their applications, Journal of Research. U.S. Geol. Surv. 4, 41–47.
Beattie, P., 1993a. The generation of uranium series disequilibria by partial melting of spinel peridotite: constraints from partitioning studies. Earth Planet. Sci. Lett. 117, 379–391.
Beattie, P., 1993b. Uranium–thorium disequilibria and partitioning on melting of garnet peridotites. Nature 363, 63–65.
Becker, H., Jochum, K.P., Carlson, R.W., 2000. Trace element fractionation during dehydration of eclogites from high-pressure terranes and the implications for element fluxes in subduction zones. Chem. Geol. 163, 65–99.
Breddam, K., 2002. Kistufell: primitive melt from the Iceland mantle plume. J. Petrol. 43, 345–373, http://dx.doi.org/10.1093/petrology/43.2.345.
Bodinier, J.L., Vasseur, G., Vernieres, J., Dupuy, C., Fabries, J., 1990. Mechanisms of mantle metasomatism: geochemical evidence from the Lherz orogenic peridotite. J. Petrol. 31, 597–628.
Borisova, A.Y., Toutain, J.P., Stefansson, A., Gouy, S., De Parseval, P., 2012. Processes controlling the 2010 Eyjafjallajökull explosive eruption. J. Geophys. Res.: Solid Earth 117, http://dx.doi.org/10.1029/2012JB009213.
Chauvel, C., Hémond, C., 2000. Melting of a complete section of recycled oceanic crust: trace element and Pb isotopic evidence from Iceland. Geochem. Geophys. Geosyst. 1, http://dx.doi.org/10.1029/1999GC000002.
Class, C., Goldstein, S.L., 1997. Plume–lithosphere interactions in the ocean basins: constraints from the source mineralogy. Earth Planet. Sci. Lett. 150, 245–260.
Debaille, V., Blichert-Toft, J., Agranier, A., Doucelance, R., Schiano, P., Albarede, F., 2006. Geochemical component relationships in MORB from the Mid-Atlantic Ridge, 22–35° N. Earth Planet. Sci. Lett. 241 (3–4), 844–862.
Debaille, V., Troennes, R.G., Brandon, A.D., Waight, T.E., Graham, D.W., Lee Cin-Ty, A., 2009. Primitive off-rift basalts from Iceland and Jan Mayen: OS-isotopic evidence for a mantle source containing enriched subcontinental lithosphere. Geochim. Cosmochim. Acta 73, 3423–3449.
Donnelly, K.E., Goldstein, S.L., Langmuir, C.H., Spiegelman, M., 2004. Origin of enriched ocean ridge basalts and implications for mantle dynamics. Earth Planet. Sci. Lett. 226, 347–366.
Dostal, J., Dupuy, C., Liotard, J.M., 1982. Geochemistry and origin of basaltic lavas from Society Islands. French Polynesia (South Central Pacific Ocean). Bull. Volcanol. 45 (1), 51–62.
Downes, H., 2007. Origin and significance of spinel and garnet pyroxenites in the shallow lithospheric mantle: ultramafic massifs in orogenic belts in Western Europe and NW Africa. Lithos 99, 1–24.
Dugmore, A.J., Newton, A.J., Smith, K.T., Mairs, K.A., 2013. Tephrochronology and the late Holocene volcanic and flood history of Eyjafjallajökull, Iceland. J. Quat. Sci. 28 (3), 237–247.
Dupuy, C., Barsczus, H.G., Liotard, J.M., Dostal, J., 1988. Trace element evidence for the origin of ocean island basalts: an example from the Austral Island (French Polynesia). Contrib. Mineral. Petrol. 98, 293–302.
Eiler, J.M., Grönvold, K., Kitchen, N., 2000. Oxygen isotope evidence for the origin of chemical variations in lavas from Theistareykir volcano in Iceland's northern volcanic zone. Earth Planet. Sci. Lett. 184, 269–286, http://dx.doi.org/10.1016/S0012-821X(00)00318-6.
Elliott, T., Blichert-Toft, J., Heumann, A., Koetsier, G., Forjaz, V., 2007. The origin of enriched mantle beneath São Miguel, Azores. Geochim. Cosmochim. Acta 71, 219–240.
Fitton, J.G., Saunders, A.D., Nrry, M.J., Hardarson, B.S., Taylor, R.N., 1997. Thermal and chemical structure of the Iceland plume. Earth Planet. Sci. Lett. 153, 197–208, http://dx.doi.org/10.1016/S0012-821X(97)00170-2.
Foulger, G.R., Anderson, D.L., 2005. A cool model for the Iceland hotspot. J. Volcanol. Geotherm. Res. 141, 1–22.
Foulger, G.R., Natland, J.H., Anderson, D.L., 2005. A source for Icelandic magmas in remelted Iapetus crust. J. Volcanol. Geotherm. Res. 141, 23–44.
Gee, M.A.M., Thirlwall, M.F., Taylor, R.N., Lowry, D., Murton, B.J., 1998. Crustal processes: major controls on Reykjanes peninsula lava chemistry, SW Iceland. J. Petrol. 39, 819–839, http://dx.doi.org/10.1093/petroj/39.5.819.
Green, T.H., Pearson, N.J., 1985. Experimental determination of REE partition coefficients between amphibole and basaltic to andesitic liquids at high pressure. Geochim. Cosmochim. Acta 49, 1465–1468, http://dx.doi.org/10.1016/0016-7037(85)90295-9.
Gudmundsson, M.T., Pedersen, R., Vogfjörd, K., Thorbjarnardóttir, B., Jakobsdóttir, S., Roberts, M.J., 2010. Eruptions of Eyjafjallajökull Volcano, Iceland. Eos Trans. AGU 91 (21), 190–191, http://dx.doi.org/10.1029/2010EO210002.
Gurenko, A.A., Chaussidon, M., 1995. Enriched and depleted primitive melts included in olivine from Icelandic tholeiites: origin by continuous melting of a single mantle column. Geochim. Cosmochim. Acta 59, 2905–2917.
Hanan, B.B., Schilling, J.-G., 1997. The dynamic evolution of the Iceland mantle plume: the lead isotope perspective. Earth Planet. Sci. Lett. 151, 43–60.
Hart, S.R., Staudigel, H., 1982. The control of alkalis and Uranium in sea-water by ocean crust alteration. Earth Planet. Sci. Lett. 58 (2), 202–212, http://dx.doi.org/10.1016/0012-821X(82)90194-7.
Hart, S.R., Dunn, T., 1993. Experimental cpx/melt partitioning of 24 trace elements. Contrib. Mineral. Petrol. 113, 1–8.
Harte, B., Hunter, R.H., Kinny, P.D., 1993. Melt geometry, movement and crystallization, in relation to mantle dykes, veins and metasomatism. Philos. Trans. R. Soc. Lond. Ser. A 342, 1–21.
Hemond, C., Arndt, N.T., Lichtenstein, U., Hofmann, A.W., Oskarsson, N., Steinthorsson, S., 1993. The heterogeneous Iceland plume: Nd–Sr–O isotopes and trace element constraints. J. Geophys. Res. 98, http://dx.doi.org/10.1029/93JB01093.
Hemond, C., Hofmann, A.L., Vlastelic, I., Nauret, F., 2006. Origin of MORB enrichment and relative trace element compatibilities along the Mid-Atlantic Ridge between 10 and 24N. Geochem. Geophys. Geosyst. 7 (12), Q12010, http://dx.doi.org/10.1029/2006GC001317.
Hoernle, K., Hauff, F., Kokfelt, T.F., Haase, K., Garbe-Shonberg, D., Werner, R., 2011. On- and off-axis chemical heterogeneities along the South Atlantic Mid-Ocean-Ridge (5–11° S): shallow or deep recycling of ocean crust and/or intraplate volcanism? Earth Planet. Sci. Lett. 306 (1–2), 86–97.
Hofmann, A.W., 1997. Mantle geochemistry: the message from oceanic volcanism. Nature 385, 219–229.
Hofmann, A.W., White, W.M., 1982. Mantle plumes from ancient oceanic crust. Earth Planet. Sci. Lett. 57, 421–436.
Humphris, S.E., Thompson, G., 1983. Geochemistry of rare earth elements in basalts from the Walvis Ridge: implications for its origin and evolution. Earth Planet. Sci. Lett. 66, 223–242.
Irving, A.J., Frey, F.A., 1984. Trace element abundances in megacrysts and their host basalts: constraints on partition coefficients and megacryst genesis. Geochim. Cosmochim. Acta 48, 1201–1221.
John, T., Scherer, E.E., Haase, K., Schenk, V., 2004. Trace element fractionation during fluid-induced eclogitization in a subducting slab: trace element and Lu–Hf–Sm–Nd isotope systematics. Earth Planet. Sci. Lett. 227, 441–456.
Kamenetsky, V.S., Everard, J.L., Crawford, A.J., Varne, R., Eggins, S.M., Lanyon, R., 2000. Enriched end-member of primitive MORB melts: petrology and geochemistry of glasses from Macquarie Island (SW Pacific). J. Petrol. 41 (3), 411–430.
Kelemen, P.B., Shimizu, N., Dunn, T., 1993. Relative depletion of niobium in some arc magmas and the continental crust: partitioning of K, Nb, La and Ce during melt/rock reaction in the upper mantle. Earth Planet. Sci. Lett. 120, 111–134.
Kokfelt, T.F., Hoernle, K., Hauff, F., Fiebig, J., Werner, R., Garbe-Schonberg, D., 2006. Combined trace element and Pb–Nd–Sr–O isotope evidence for recycled oceanic crust (upper and lower) in the Iceland mantle plume. J. Petrol. 47, 1705–1749.
Koorneef, J.M., Stracke, A., Bourdon, B., Meier, M.A., Jochum, K.P., Stoll, B., Gronvold, K., 2012. Melting of a two-component source beneath Iceland. J. Petrol. 53 (1), 127–157.
LaTourrette, T.Z., Hervig, R.L., Holloway, J.R., 1995. Trace element partitioning between amphibole, phlogopite, and basanite melt. Earth Planet. Sci. Lett. 135, 13–30.
Le Maitre, R.W., 2002. A Classification of Igneous Rocks and Glossary of Terms. Cambridge University Press, pp. 236.
Mallick, S., Dick, H.J.B., Sachi-Kocher, A., Salters, V.J.M., 2014. Isotope and trace element insights into heterogeneity of subridge mantle. Geochem. Geophys. Geosyst. 15 (6), 2438–2453.
McCulloch, M.T., Gamble, J.A., 1991. Geochemical and geodynamical constraints on subduction zone magmatism. Earth Planet. Sci. Lett. 102, 358–374.
McDade, P., Blundy, J.D., Wood, B.J., 2003. Trace element partitioning on the Tinaquillo lherzolite solidus at 1.5 GPa. Phys. Earth Planet. Interior 139, 129–147.
McDonough, W.F., Sun, S.S., 1995. The composition of the Earth. Chem. Geol. 120, 223–253.
Moune, S., Sigmarsson, O., Schiano, P., Thordarson, T., Keiding, J.K., 2012. Melt inclusion constraints on the magma source of Eyjafjallajökull 2010 flank eruption. J. Geophys. Res.: Solid Earth 117, B00C07, http://dx.doi.org/10.1029/2011JB008718.
Mysen, B., 1979. Trace-element partitioning between garnet peridotite minerals and water-rich vapor: experimental data from 5 to 30 kbar. Am. Mineral. 64, 274–287.
Morris, E.M., Pasteris, J.D., 1987. Mantle metasomatism and alkaline magmatism. Geological Society of America, Special Papers, vol. 215.
Nielson, J.E., Noller, J.S., 1987. Processes of mantle metasomatism; Constraints from observations of composite peridotite xenoliths. In: Morris, E.M., Pasteris, J.D. (Eds.), Mantle Metasomatism and Alkaline Magmatism Special Papers. Geological Society of America, vol. 215, pp. 61–76.
Nielson, J.E., Wilshire, H.G., 1993. Magma transport and metasomatism in the mantle: a critical review of current geochemical models. Am. Mineral. 78, 1117–1134.
Niu, Y., Waggoner, D.G., Sinton, J.M., Mahoney, J.J., 1996. Mantle source heterogeneity and melting processes beneath seafloor spreading centers: The East Pacific Rise, 18°–19° S. J. Geophys. Res.: Solid Earth 101 (12), 27711–27733.
Niu, Y., Bideau, D., Hèkinian, R., Batiza, R., 2001. Mantle compositional control on the extent of mantle melting, crust production, gravity anomaly, ridge morphology, and ridge segmentation: a case study at the Mid-Atlantic Ridge 33–35° N. Earth Planet. Sci. Lett. 186, 383–399.
Niu, Y., O'Hara, M.J., 2003. Origin of ocean island basalts: a new perspective from petrology, geochemistry, and mineral physics considerations. J. Geophys. Res. 108, 2209, http://dx.doi.org/10.1029/2002JB002048.

Palacz, Z., Saunders, A.D., 1986. Coupled trace element and isotope enrichment in the Cook-Austral-Samoa islands, southwest Pacific. Earth Planet. Sci. Lett. 79, 270–280.
Peacock, M.A., 1925. A contribution to the petrography of Iceland. Trans. Geol. Soc. Glasgow 17, 271–333.
Peacock, M.A., 1926. The petrology of Iceland. I. The basic tuffs. Trans. R. Soc. Edinburgh 55, 51–76.
Pedersen, R., Sigmundsson, F., 2004. InSAR based sill model links spatially offset areas of deformation and seismicity for the 1994 unrest episode at Eyjafjallajökull volcano. Iceland Geophys. Res. Lett. 31 (14), L14610, http://dx.doi.org/10.1029/2004GL020368.
Pedersen, R., Sigmundsson, F., 2006. Temporal development of the 1999 intrusive episode in the Eyjafjallajökull volcano, Iceland, derived from InSAR images. Bull. Volcanol. 68 (4), 377–393.
Pilet, S., Baker, M.B., Stolper, E.M., 2008. Metasomatized lithosphere and the origin of alkaline lavas. Science 320, 916–919.
Pilet, S., Baker, M.B., Müntener, O., Stolper, E.M., 2011. Monte Carlo Simulations of metasomatic enrichment in the lithosphere and implications for the source of alkaline basalts. J. Petrol. 52, 1415–1442, http://dx.doi.org/10.1093/petrology/egr007.
Salters, V.J.M., 1996. The generation of mid-ocean ridge basalts from the Hf and Nd isotope perspective. Earth Planet. Sci. Lett. 141 (1–4), 109–123.
Salters, V.J.M., Stracke, A., 2004. Composition of the depleted mantle. Geochem. Geophys. Geosyst. 5 (5), Article number Q05004.
Salters, V.J.M., Mallick, S., Hart, S.R., Langmuir, C.E., Stracke, A., 2011. Domains of depleted mantle: new evidence from hafnium and neodymium isotopes. Geochem. Geophys. Geosyst. 12 (8), Article number Q08001.
Schilling, J.G., 1973a. Iceland mantle plume: geochemical study of Reykjanes Ridge. Nature 242, 565–571.
Schilling, J.G., 1973b. Iceland mantle plume. Nature 246, 141–143.
Schilling, J.G., 1986. Geochemical and isotopic variation along the Mid-Atlantic Ridge axis from 79° N to 0° N. In: Vogt, P.R., Tucholke, B.E. (Eds.), The Geology of North America, Volume M: The Western North Atlantic Region. Geological Society of America, Boulder, CO, pp. 137–156.
Sigmarsson, O., Maclennan, J., Carpentier, M., 2008. Geochemistry of igneous rocks in Iceland: a review. Joekull 58, 139–160.
Sigmarsson, O., Vlastelic, I., Devidal, J., 2010. Trace-element variations reveal dynamic magma mixing during the 2010 eruption of Eyjafjallajokull, Iceland. Fall Meeting AGU San Francisco, abstract V21F-0VF4.
Sigmarsson, O., Vlastelic, I., Andreasen, R., Bindeman, I., Devidal, J.L., Moune, S., Keiding, J.K., Larsen, G., Höskuldsson, A., Thordarson, T., 2011. Dynamic magma mixing revealed by the 2010 Eyjafjallajökull eruption. Solid Earth 2, 271–281, http://dx.doi.org/10.5194/se-2-271-2011.
Sigmundsson, F., Hreinsdóttir, S., Hooper, A., Árnadóttir, T., Pedersen, R., Roberts, M.J., Óskarsson, N., Auriac, A., Decriem, J., Einarsson, P., Geirsson, H., Hensch, M., Ófeigsson, B.G., Sturkell, E., Sveinbjörnsson, H., Feigl, K.L., 2010. Intrusion triggering of the 2010 Eyjafjallajökull explosive eruption. Nature 468, 426–432.
Skovgaard, A.C., Storey, M., Baker, J., Blusztajn, J., Hart, S.R., 2001. Osmium-oxygen isotopic evidence for a recycled and strongly depleted component in the Iceland mantle plume. Earth Planet. Sci. Lett. 194, 259–275.
Spera, F.J., Bohrson, W.A., Christy, B.T., Ghiorso, M.K., 2007. Partitioning of trace elements among coexisting crystals, melt, and supercritical fluid during isobaric crystallization and melting. Am. Mineral. 92, 1881–1898.
Staudigel, H., Davies, G.R., Hart, S.R., Marchant, K.M., Smith, B.M., 1995. Large scale isotopic Sr, Nd and O isotopic anatomy of altered oceanic crust: DSDP/ODP sites 417/418. Earth Planet. Sci. Lett. 130, 169–185, http://dx.doi.org/10.1016/0012-821X(94)00263-X.
Staudigel, H., Plank, T., White, B., Schmincke, H.U., 1996. Geochemical fluxes during seafloor alteration of the upper oceanic crust: DSDP sites 417–418. In: Bebout, G.E., Scholl, D.W., Kirby, S.H., Platt, J.P. (Eds.), Subduction top to bottom. Geophysical Monograph, 96. American Geophysical Union, Washington, DC, pp. 19–38.
Storey, M., Saunders, A.D., Tarney, J., Leat, P., Thirlwall, M.F., Thompson, R.N., Menzies, M.A., Marriner, G.F., 1988. Geochemical evidence for plume-mantle interactions beneath Kerguelen and Heard Islands, Indian Ocean. Nature 336, 371–374.
Stracke, A., Bizimis, M., Salters, V.J.M., 2003. Recycling oceanic crust: quantitative constraints. Geochem. Geophys. Geosyst. 4 (3), article number 8003.
Stracke, A., Hofmann, A.L., Hart, S.R., 2005. FOZO, HIMU and the rest of the mantle zoo. Geochem. Geophys. Geosyst. 6 (5), article number Q05007.
Sturkell, E., Sigmundsson, F., Einarsson, P., 2003. Recent unrest and magma movements at Eyjafjallajokull and Katla volcanoes, Iceland. J. Geophys. Res.: Solid Earth 108, 2369, http://dx.doi.org/10.1029/2001JB000917.
Sun, S.S., Tatsumoto, M., Schilling, J.G., 1975. Mantle plume mixing along the Reykjanes Ridge Axis: lead isotopic evidence. Science 190, 143–147.
Tatsumi, Y., Kogiso, T., 2003. The subduction factory: its role in the evolution of the Earth's crust and mantle. Geol. Soc. Lond. Spec. Publ. 219, 55–80, http://dx.doi.org/10.1144/GSL.SP.2003.219.01.03.
Thordarson, T., Larsen, G., 2007. Volcanism in Iceland in historical time: volcano types, eruption styles and eruptive history. J. Geodyn. 43, 118–152.
Thirlwall, M.F., Gee, M.A.M., Taylor, R.N., Murton, B.J., 2004. Mantle components in Iceland and adjacent ridges investigated using double-spike Pb isotope ratios. Geochim. Cosmochim. Acta 68, 361–386, http://dx.doi.org/10.1016/S0016-7037(03)00424-1.
Thirlwall, M.F., Gee, M.A.M., Lowry, D., Mattey, D.P., Murton, B.J., Taylor, R.N., 2006. Low $\delta^{18}O$ in the Icelandic mantle and its origins: evidence from Reykjanes Ridge and Icelandic lavas. Geochim. Cosmochim. Acta 70, 993–1019, http://dx.doi.org/10.1016/j.gca.2005.09.008.
Viccaro, M., Cristofolini, R., 2008. Nature of mantle heterogeneity and its role in the short-term geochemical and volcanological evolution of Mt. Etna (Italy). Lithos 105, 272–288.
Viccaro, M., Nicotra, E., Millar, I.L., Cristofolini, R., 2011. The magma source at Mount Etna volcano: perspectives from the Hf isotope composition of historic and recent lavas. Chem. Geol. 281, 343–351.
Weaver, B.L., 1991. The origin of ocean island basalt end-member compositions: trace element and isotopic constraints. Earth Planet. Sci. Lett. 104, 381–397.
Willbold, M., Stracke, A., 2006. Trace element composition of mantle end-members: implications for recycling of oceanic and upper and lower continental crust. Geochem. Geophys. Geosyst. 7 (4), http://dx.doi.org/10.1029/2005GC001005.
Wilshire, H.G., 1987. A model of mantle metasomatism. In: Morris, E.M., Pasteris, J.D. (Eds.), Mantle Metasomatism and Alkaline Magmatism. Geological Society of America, Special Papers, vol. 215, pp. 47–60.
Wolfe, C.J., Bjarnason, I.T., VanDecar, J.C., Salomon, S.C., 1997. Seismic structure of the Iceland mantle plume. Nature 385, 245–247.
Workman, R.K., Hart, S.R., Jackson, M., Regelous, M., Farley, K.A., Blusztajn, J., Kurz, M., Staudigel, H., 2004. Recycled metasomatized lithosphere as the origin of the enriched mantle II (EM2) end-member: evidence from the Samoan Volcanic Chain. Geochem. Geophys. Geosyst. 5, Q04008, http://dx.doi.org/10.1029/2003GC000623.
Workman, R.K., Hart, S.R., 2005. Major and trace element composition of the depleted MORB mantle (DMM). Earth Planet. Sci. Lett. 231, 53–72.
Zindler, A., Hart, S., 1986. Chemical geodynamics. Annu. Rev. Earth Planet. Sci. 14, 493–571.